

# We are IntechOpen, the world's leading publisher of Open Access books Built by scientists, for scientists

6,900

Open access books available

186,000

International authors and editors

200M

Downloads

Our authors are among the

154

Countries delivered to

TOP 1%

most cited scientists

12.2%

Contributors from top 500 universities



WEB OF SCIENCE™

Selection of our books indexed in the Book Citation Index  
in Web of Science™ Core Collection (BKCI)

Interested in publishing with us?  
Contact [book.department@intechopen.com](mailto:book.department@intechopen.com)

Numbers displayed above are based on latest data collected.  
For more information visit [www.intechopen.com](http://www.intechopen.com)



# Time-Dependent Behavior of Rock Materials

*Chrysothemis Paraskevopoulou*

## Abstract

Understanding the geomechanical behavior of a geological model is still an on-going challenge for engineers and scientists. More challenges arise when considering the long-term behavior of rock materials, especially when exposed to environments that enable time-dependent processes to occur and govern overall behavior. The latter is essential in underground projects such as nuclear waste repositories. The lifespan can exceed one million years or other openings where the project's lifetime and sustainability are the critical design parameter. In such cases, progressive rock mass deformation that can lead to instabilities, time-dependent overloading of support and delayed failure are considered the product of time-dependent phenomena. Understanding and predicting the overall impact of such phenomena aims to achieve design optimization, avoiding delivery delays and thus cost overruns. This chapter provides more insight into the time-dependent behavior of rocks. Simultaneously, the emphasis is given to investigating and analyzing creep deformation and time-dependent stress relaxation phenomenon at the laboratory scale, and in-depth analyses are presented. This work further develops the understanding of these phenomena, and practical yet scientific tools for estimating and predicting the long-term strength and the maximum stress relaxation of rock materials is presented. The work presented in this chapter advances the scientific understanding of time-dependent rock, and rock mass behavior increases the awareness of how such phenomena are captured numerically and lays out a framework for dealing with such deformations when predicting tunnel deformations.

**Keywords:** time-dependent behavior, long-term behavior, long-term strength, creep, stress-relaxation, strength-degradation

## 1. Introduction

Rock engineering and tunneling are considered to be three-dimensional problem. In practice, the short-term mechanical performance is of primary focus in design as design and characterization parameters and data are derived from short-term testing. Challenges and implications can be formed when performance over time and long-term behavior is taken into consideration. Current design methodologies used in underground structures and tunneling projects are commonly solely based on the static response of the surrounding ground neglecting the long-term time-dependent behavior that can affect the overall structure's performance and the construction process [1, 2]. The latter can cause difficulties when attempting to understand the governing mechanisms in rock materials where time-dependent phenomena such as creep and stress relaxation can occur [3, 4]. When these processes are excluded or

neglected during the design process, incorrect results and unsound conclusions are derived. These can involve support requirements and excavation methods employed, impacting the construction, the maintenance cost of the tunnel, and in the worst case, may even cause safety issues [5–8].

Strength-degradation is considered highly important in underground applications such as low, intermediate and high-level nuclear waste. The time-dependent strength decrease deteriorates the overall lifetime of the underground opening [9]. This lifetime span can range from 100,000 to 1,000,000 years which significantly exceeds the typical 100-year lifetime of underground projects. It is evident, thus, the reason why there is a need to investigate from micro to macro-scale further the long-term behavior of rock materials that could be used as host-rocks for such applications.

This Chapter aims to provide more insight into rock materials’ time-dependent behavior by addressing the mechanisms involved and highlighting the associated implications for both scientific and practical applications. In this work, both experimental laboratory testing and numerical analyses are employed to examine the time-dependent mechanisms and rocks’ response under different boundary conditions while introducing a different perspective for analyzing and predicting the intact rock’s time-dependent behavior of the rock mass behavior in underground environments. A time-dependent response such as creep, squeezing, swelling, stress relaxation, and strength degradation of the rock mass can occur during both the construction and the maintenance of underground openings depending on the in situ conditions that control the mechanical behavior shown in **Figure 1**.

It has been observed that an often misconception is the assumption that time-dependent phenomena only act individually. However, this assumption can yield unsound estimations and erroneous conclusions. These phenomena may share the same (or similar) mechanisms given the existing in situ conditions can take place either in series or even simultaneously. Therefore, the overall observed displacement on the tunnel wall can result from different phenomena acting together. The selection of an appropriate constitutive model to examine the mechanical behavior of rock material overtime is required. The ability of such models to capture and simulate time-dependent behavior is illustrated in **Figure 2**.

The time-effect can cause different behavioral patterns depending on the underground construction project’s site-specific conditions; the selection of the

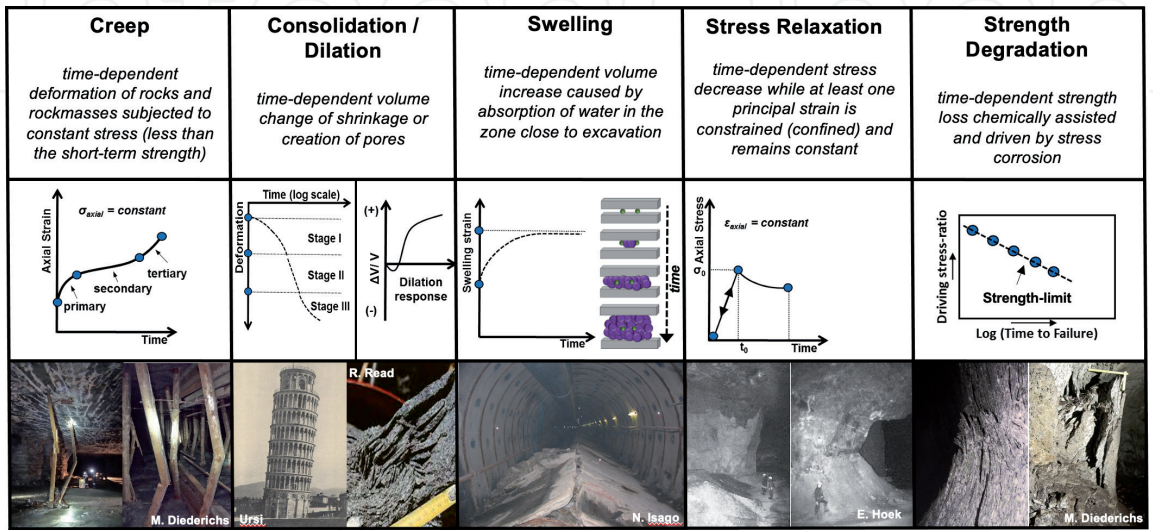


**Figure 1.** Examples of time-dependent phenomena, the behavioral response with time and a description of the phenomena encountered in rock tunneling.

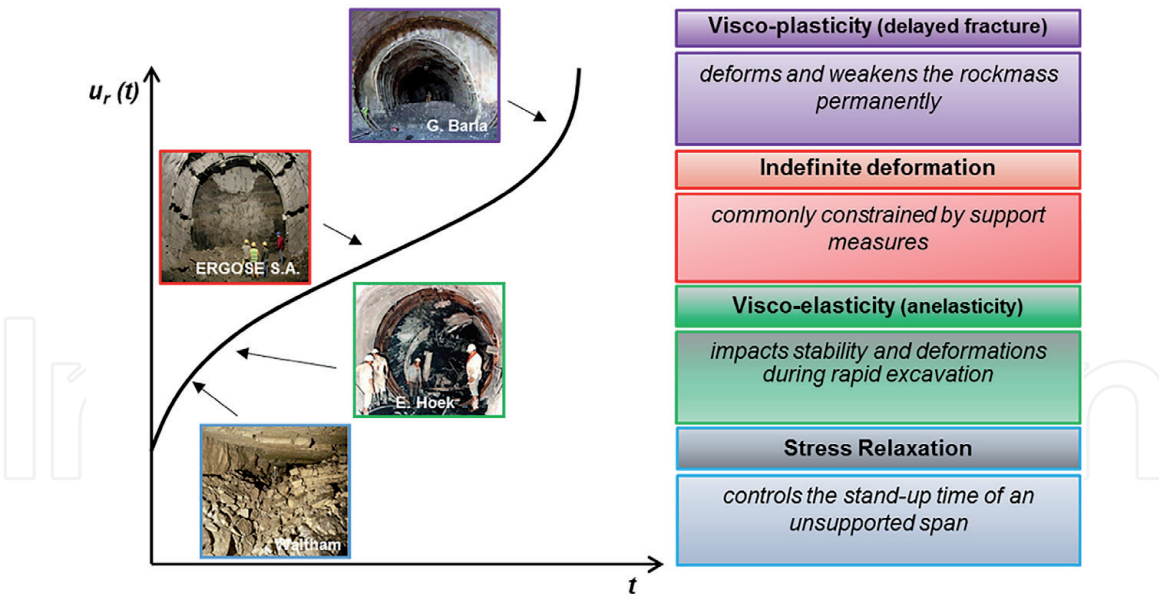


**Figure 2.**  
 Examples of reported failures and mechanisms associated with time-dependent behavior; where  $t$  refers to time and  $u_r(t)$  to the radial displacements observed in the tunnel walls over time.

appropriate model to simulate the desired mechanical response is crucial. For instance, stress relaxation usually occurs near the newly exposed walls after the tunnel face excavation. The visco-elasticity (or anelasticity) can cause implications during rapid excavation (i.e., TBM). The indefinite deformation usually observed in more ductile materials can result from the deterioration of the support system. In this case, different support measures (i.e., yielding support systems) should be undertaken where the on-going deformation will be allowed to take place. Visco-plasticity or delayed fracturing can permanently damage the rock mass after initial construction, requiring redesigning the initial tunnel design. These examples show the importance of using the appropriate model to simulate the real conditions as closely as possible and estimate how the rock mass will behave over time.

## 2. Theoretical and practical background

Different rocks and rock masses respond in different ways over time. The main factor that controls their behavior is geology. The mineralogical content and the geological structure impact rocks' mechanical behavior; ultimately, the stress regime and the environmental conditions also influence the rock materials' behavior. **Figure 3** provides a roadmap on the material's anticipated mechanical behavior grouped into ductile or brittle behavior based on the conditions the material is initially formed. In general, as the temperature and confining pressure increase, the rock transitions from brittle to ductile (**Figure 3a**). Brittle materials tend to abruptly fail as the stress approaches their short-term strength, and as such, they absorb less energy. In contrast, ductile materials can sustain an applied stress state through more deformation (**Figure 3b** and **c**). When ductile materials (i.e. rock salt or potash) are subjected to constant differential stress below their nominal yield strength, they can behave as visco-elastic materials and further deform as time elapses (**Figure 3d** and **e**). In contrast, brittle materials (i.e., granite or limestone) under similar stress conditions may only exhibit micro-crack damage with progressive crack propagation that results in the eventual interaction of the previously isolated microcracks, which leads to sudden failure (**Figure 3d** and **e**).

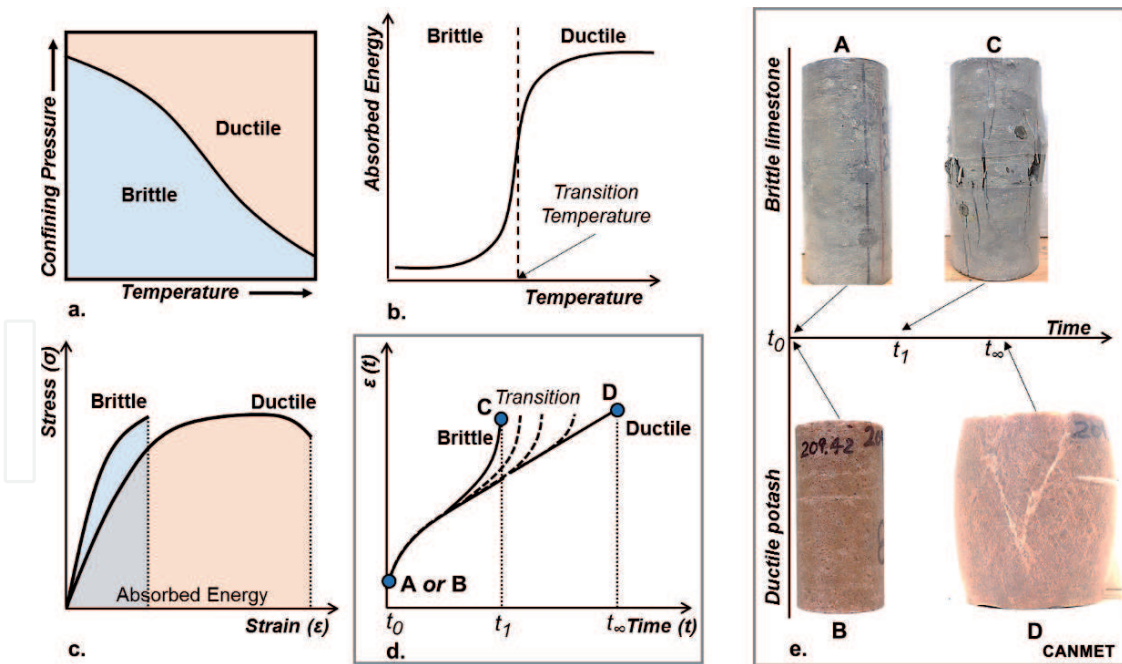


**Figure 3.**

Schematic illustration and comparison between brittle and ductile rock materials, (a) transition from brittle to ductile behavior according to confining pressure and temperature conditions; (b) absorbed energy and temperature; (c) general stress – Strain behavior of brittle and ductile materials; (d) strain- rate and time relationship of brittle and ductile materials subjected to constant stress exhibiting creep, and (e) examples of brittle limestone and ductile potash before and after static load (creep) tests.

## 2.1 Time-dependent phenomena

Time-dependency refers to the deformation of rock (or other materials) over time. Mechanisms deforming or weakening the rock mass over time are called time-dependent phenomena. Since the late 1930s, researchers started investigating the effect of time in rock behavior, trying to apply the theory of creep widely studied and reported on metals [10] to rock behavior. It was not until 1939 when Griggs [11] undertook laboratory experiments to examine the phenomenon of creep of rocks. He constructed two apparatus and performed tests on limestone, anhydrite, shale and chalk. He also examined recrystallization under creep conditions at high pressure. At the excavation scale, addressing the effect of time in tunneling and mining engineering has been studied since the 1950s. Researchers introduced the idea of ‘stand-up time’ in tunnel stability. The ‘stand up time’, a reflection of time-dependent weakening, was also included in the rock mass classification systems [12–14], emphasizing time and its effects by producing charts illustrating the time frame of stable unsupported spans. Since the 1960s many researchers [15–25] have investigated the influence of time on the long-term strength of rock by performing laboratory testing on rock samples, typically using static load (creep) tests by sustaining a constant stress condition. Creep phenomenon is most commonly applied to the study of soft, mono-mineralic rocks such as halite, potash, and limestone [26]. Following this practice, new constitutive and numerical time-dependent models were introduced based on the experimental results and data [27–31]. These models attempt to capture and reproduce the behavior of laboratory tests on the rocks, including time.

In practice, as previously mentioned, there is often a miscomprehension and misinterpretation of the different time-dependent phenomena and the mechanisms acting and resulting in weakening rock and the rock mass over time [9]. This section serves as an attempt to redefine and describe the various mechanisms that can appear to be time-dependent under the appropriate conditions using the composite

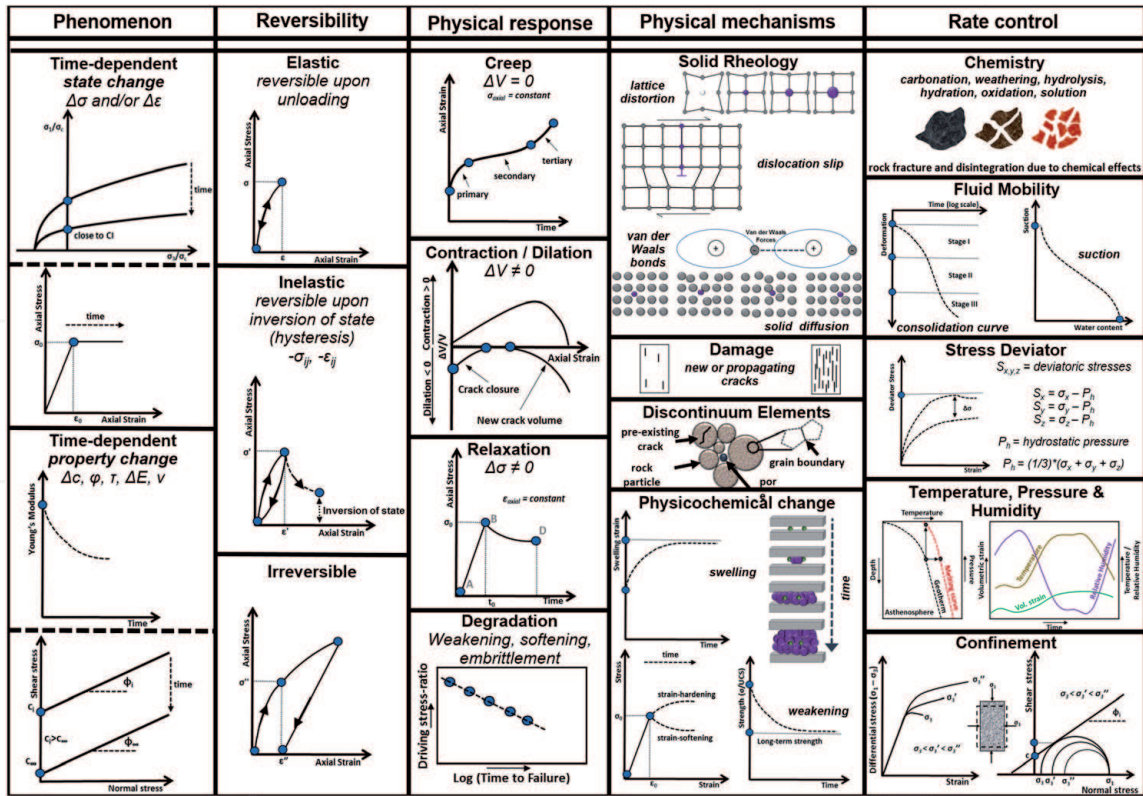


**Figure 4.** Nomenclature, defining time-dependent phenomena and the conditions and mechanisms that affect and govern the rock behavior [9].

nomenclature shown in **Figure 4**. The phenomenon can be either due to a state-change (i.e. stress decrease) or a property-change (i.e. decrease in cohesion). These changes can be further categorized according to their reversibility or recoverability as elastic, inelastic, and irreversible and may increase to visco-elastic or visco-plastic strains. The physical response can be represented as creep (shear strain), contraction or dilation (volumetric strains) over time, as well as relaxation (reduction in shear stress under sustained strain) and degradation (strength loss) depending on loading and boundary conditions. The micro-mechanical mechanisms tend to vary according to the boundary conditions. For instance, the solid rheology (e.g. lattice distortion, dislocation slip, van der Vaal's bonds and/or solid diffusion) may be damaged by new cracks that initiate or pre-existing ones propagate while pores, grain boundaries, and pre-existing cracks creating discontinuum elements. Besides, the physicochemical changes can be temporal, rheological, and chemical alterations in the micro-scale, leading to swelling, weakening, strain-softening, and hardening. The rate and the magnitude of the time-dependent performance of rock materials are controlled by other environmental, physical, and loading conditions (e.g. temperature, pressure, humidity, and confinement).

Time-dependent phenomena can be a combination of many factors that can result in various physical responses and act either simultaneously or individually. Differentiating and recognizing these phenomena can be a complicated process, and all components in **Figure 4** should be taken into account.

The overall physical response can be a combination/integration of the mechanisms that influence the long-term behavior of intact rock and rock masses and include:

- creep during which visco-elastic behavior governs where time-dependent, inelastic strains and ‘indefinite’ deformation occur and/or visco-plastic yield where time-dependent plastic strains occur that lead to permanent deformation.

- dilation or contraction where volume change takes place over time usually caused by the change of stress resulting in the propagation and interaction of cracks (dilation) or the closure of the existing ones (contraction).
- relaxation where the reduction of the stress with time under sustained strain is controlled by the internal creep processes aimed at relieving the stored elastic energy
- mechanical property degradation where strength and/or stiffness change due to damage processes that accompany or occur as a result of the above phenomenon.

## 2.2 Time-dependent laboratory tests

Time-dependent behavior of rock materials is usually investigated in the lab-scale by performing static load (creep) and stress relaxation tests which can be done in uniaxial and triaxial compressive conditions.

### 2.2.1 Relaxation tests

Relaxation is defined as stress (or load) decrease over time when the deformation (or strain) is kept constant. Commonly, the axis on which the stress is applied (i.e. axial stress used) determines the deformation's axes that are maintained constant (i.e. axial strain – constant). It has been observed that relaxation behavior is related not only to time-dependent phenomena like creep but also to time-dependent damage evolution of new or pre-existing cracks growth and evolution in the specimen that initiates during loading [9, 32, 33].

**Figure 5** shows the stages during a stress relaxation test from A to C. The rock is initially loaded in the axial direction up to point A, which is considered the strain threshold at which the applied strain is held constant (points A to C). In this regard, these tests are often referred to as strain-controlled. Overtime, existing cracks and/or new cracks are formed and propagated at this strain threshold, contributing to the observed stress decrease (relaxation). When this stress relaxation reaches an asymptote (no further decrease is observed), the test is terminated, which implies that crack growth stabilization is achieved [19].

It should be stated that suggested standard test guidelines on relaxation tests on rock samples are not provided by ISRM. However, there are guidelines provided by ASTM [34] for relaxation testing performed on man-made materials and structures. In section 3.2 this standard has been adopted and adjusted for rock relaxation testing.

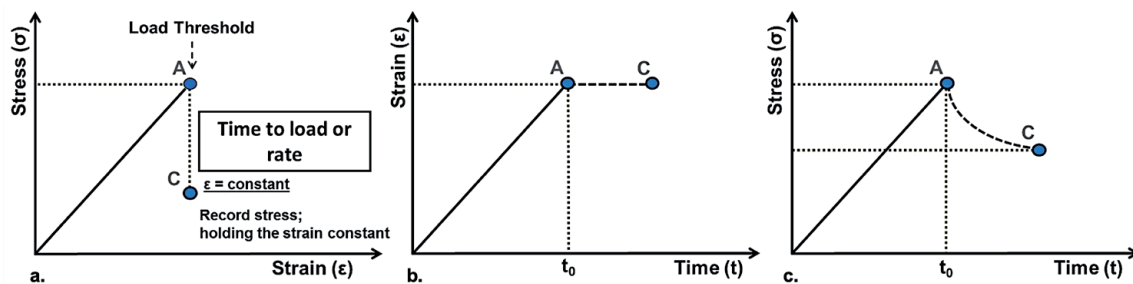


**Figure 5.** Relaxation test: (a) stress–strain response, (b) strain–time response, (c) stress–time response.

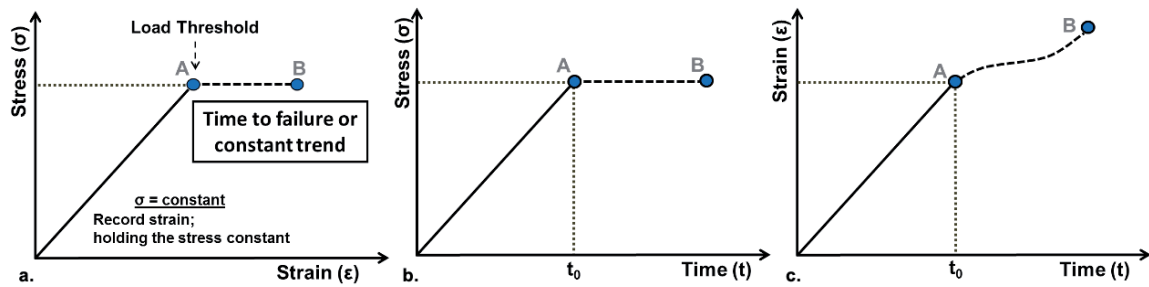


**Figure 6.**  
 Static load test: (a) stress–strain response, (b) stress–time response, (c) strain–time response.

### 2.2.2 Static load tests

To investigate creep, this time-dependent deformation of materials subjected to constant load or stress less than its short-term strength, static load tests are performed. In materials, here is a minimum load or stress, which enables them to undergo creep behavior, below which no creep is observed [9, 35, 36]. Elevated differential stress triggers the deformation of crystal lattices, leading to strain-  
 ing of the minerals, potentially microcracking, and eventually measurable strain of the rock element. **Figure 6** presents a typical stress–strain–time response of a (uniaxial) creep test. The rock sample is loaded until point A, the stress threshold where it is held constant. Over time the strain increases at different rates up to point B, where failure occurs. This test is usually referred to as load-controlled or stress-controlled tests.

Failure of the specimen usually denoted the completion of the test. However, many static load tests are terminated when a constant strain-rate is achieved, inferring the transition to the secondary stage of creep. For static load tests, ISRM [37] has suggested standard guidelines.

## 2.3 Time-dependent models

The time-dependent mechanisms are usually investigated by developing analytical methods adopting rheological models (comprising mechanical analogues) and empirical models based on laboratory testing data. Specifically, creep behavior is mathematically represented by the Burgers model. This model combines two simplified linear visco-elastic mechanical analogues in series: the Kelvin and the Maxwell that simulate a delayed manifestation of a static response due to boundary conditions alteration and a continued strain rate relaxation overtime under static boundary conditions, respectively shown in **Figure 7**.

Deformation that occurs at constant loading condition through time can be expressed using Eq. (1) [38], where:  $\varepsilon_1$  is the axial strain,  $\sigma_1$  is the constant axial stress,  $K$  is the bulk modulus,  $\eta_K$  is Kelvin's model viscosity,  $\eta_M$  is Maxwell's model viscosity,  $G_K$  is Kelvin's shear modulus,  $G_M$  is Maxwell's shear modulus.  $\eta_K$ ,  $\eta_M$ ,  $G_K$ ,  $G_M$  are the visco-elastic parameters and are considered properties of the rock.

$$\varepsilon_1(t) = \frac{2\sigma_1}{9K} + \frac{\sigma_1}{3G_M} + \frac{\sigma_1}{3G_K} - \frac{\sigma_1}{3G_K} e^{-\left(\frac{G_K}{\eta_K}t\right)} \quad (1)$$

During stress relaxation, the strain-state is controlled and remains constant, thus rearranging Eq. (1) for a constant strain component, the material's stress state is changing according to Eq. (2).

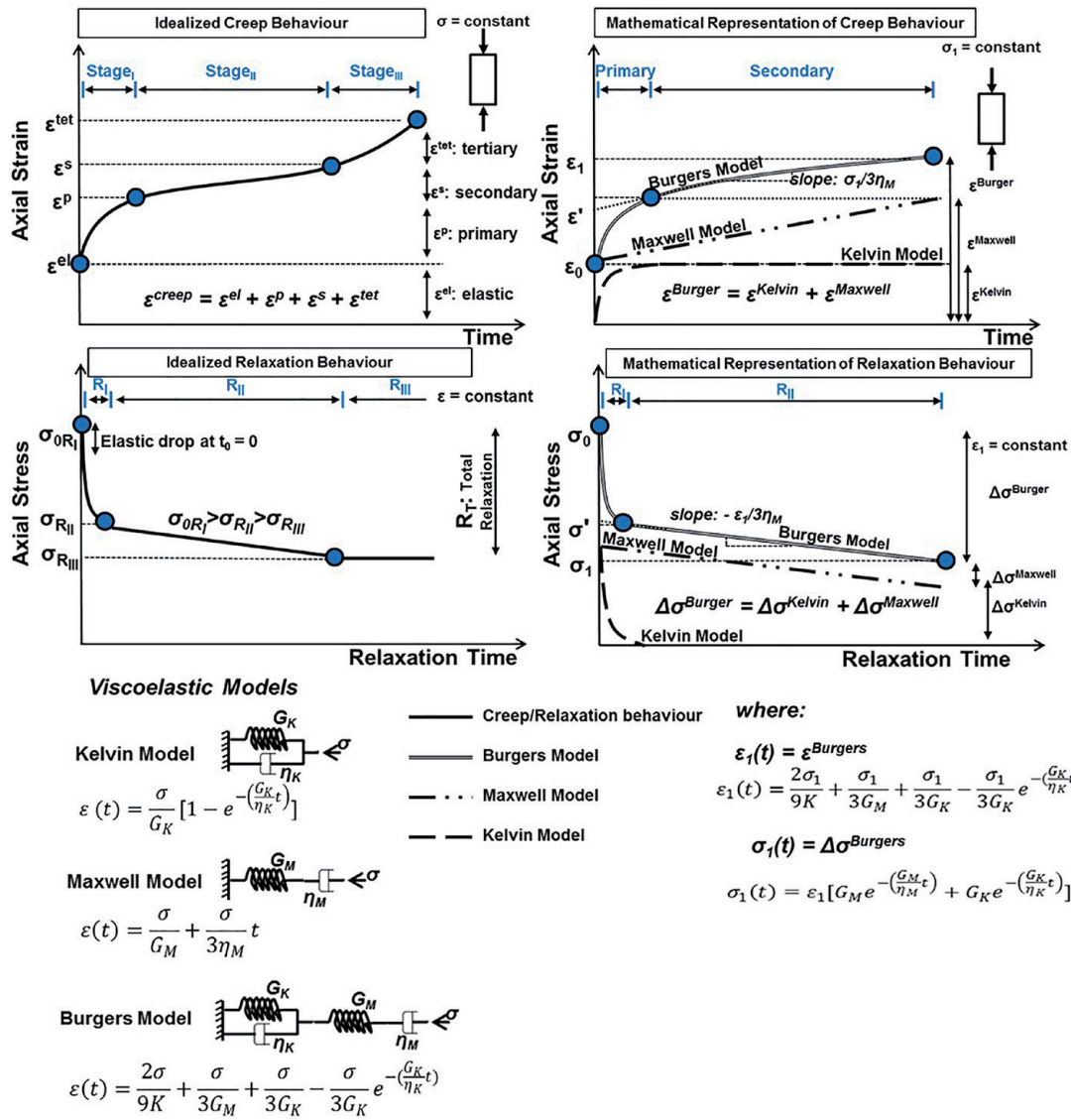


**Figure 7.** Idealized creep and relaxation behavioral curves and the equivalent visco-elastic components in the Burgers model.

$$\sigma_1(t) = \varepsilon_1 \left[ G_M e^{-\left(\frac{G_M}{\eta_M} t\right)} + G_K e^{-\left(\frac{G_K}{\eta_K} t\right)} \right] \quad (2)$$

Goodman's [38] approach is usually adopted to derive the Burgers model parameters by curve fitting laboratory creep testing results. Using a similar approach for determining parameters and assuming that the material's behavior can be represented by the linear visco-elastic Burgers body in unconfined compression [33] found that the same parameters (i.e. viscosities and shear moduli) can be also derived from stress relaxation tests, (Figure 7).

In reality and embedded in this mathematical concept are the three stages of creep that follow the instantaneous response (0th stage) to changed boundary conditions resulting to a constant stress-state as follows:

- 1st stage or primary or transient creep where the delayed adjustment to a new equilibrium state takes place through visco-elastic (reversible) deformation, and may be accompanied by some irreversible behavior, resulting in strain accumulation with decreasing rate over time. This stage is commonly simulated with the Kelvin model analogue.

- 2nd stage or secondary creep where the material exhibits a consistent strain accumulation rate over time accompanied by inelastic distortion. The duration or even existence of this stage can vary depending on the ability of the rock type to transition from ductile to more brittle materials. The Maxwell visco-elastic model is commonly used to phenomenologically represent this stage.
- 3rd stage or tertiary creep where strong non-linear or accelerating strains occur (typically driving the material to rupture) due to strain-driven weakening, chemically related strength degradation and/or interaction of growing cracks. Visco-plastic models and/or so-called stress corrosion models are used to simulate tertiary creep.

A combination of Kelvin and Maxwell model components is referred to as the Burgers model which can be used to simulate stages 1 and 2 in combination.

2.4 Damage evolution and failure in brittle rocks

Over (geological) time, ductile deformation processes involve continuum mechanisms such as dislocation slip or migration of atomic vacancies within crystals resulting in distortion (pure or simple shear strain) [39]. However, in brittle materials, failure is controlled and governed by progressive damage driven by the pre-existing and new cracks initiation and evolution in the maximum load direction [40, 41]. **Figure 8** presents the four distinct stages during brittle deformability and failure: (i) closure of pre-existing cracks; (ii) linear elastic behavior; (iii) stable crack growth; and (iv) unstable crack growth, which leads to failure and the peak strength.

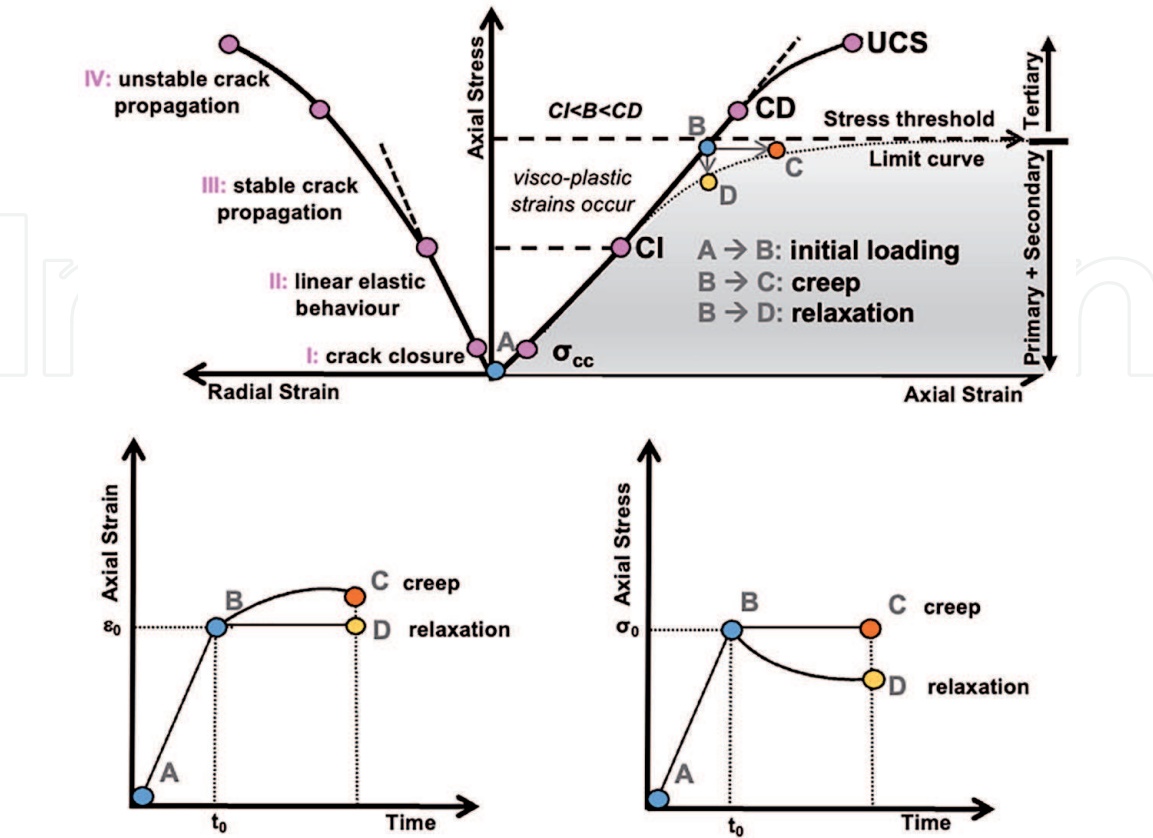


Figure 8.  
Stress - strain response of brittle rock deformability and time-dependent behavior of creep and/or relaxation.

Stress–strain curves for brittle rocks can be used to determine the: (i) crack initiation stress (CI); (ii) critical damage stress or axial yield stress (CD), and (iii) uniaxial compressive strength (UCS). While UCS strength can inhibit the loading rate and testing procedure influences, CD is the true upper bound yield strength when obtained in the lab, according to ISRM [42] standards [43]. In the limit CD, can drop in situ to the lower bound defined by CI. This lower bound is relatively insensitive to moderate pre-existing damage and other influences and is found to be 30–50% of standard UCS in brittle rocks as measured in the lab [44] or by in situ back analysis [45]. Below CI, the sample is genuinely elastic, with no new damage occurring in the sample.

### 3. Laboratory testing program and methods

Laboratory tests were performed in two types of limestone to examine time-effects in brittle materials. The selected Jurassic limestone comes from a quarry north of Zurich, Switzerland (**Figure 9a**). The Cobourg limestone (**Figure 9b**) comes from the Bowmanville quarry near Bowmanville, Ontario, Canada. It should be noted that sample preparation were conducted according to ISRM [42].

Unconfined Compressive Strength (UCS) tests were conducted on 10 cylindrical samples of Jurassic and 9 of Cobourg. Relaxation tests were conducted on 19 Jurassic and 16 Cobourg samples. Static Load tests were performed on 12 Jurassic and 5 Cobourg samples.

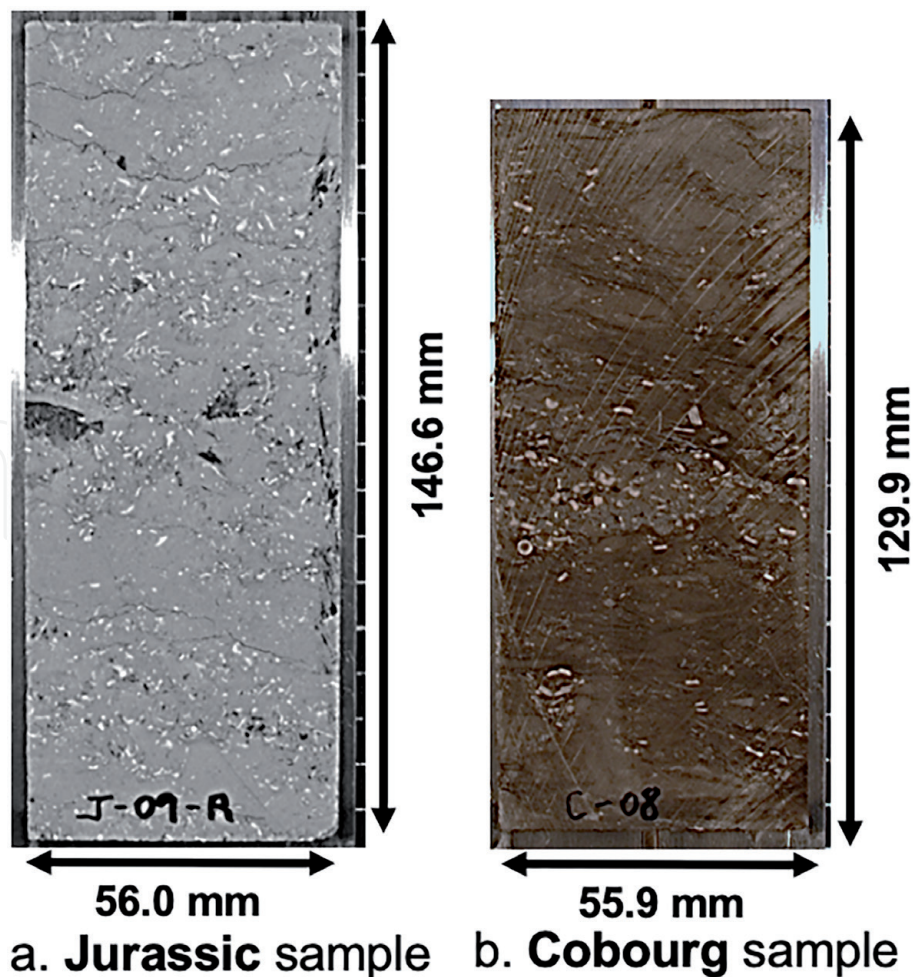


**Figure 9.**  
Samples of (a) Jurassic limestone, (b) Cobourg limestone.

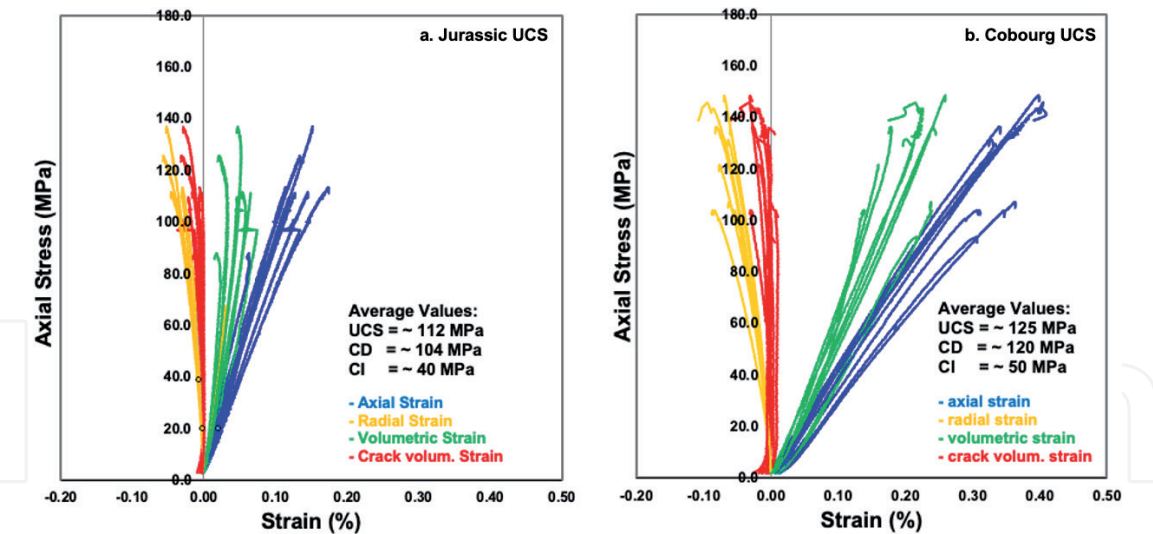


**Figure 10.**  
*Stress-strain response of limestone: (a) Jurassic samples and (b) Cobourg samples tested in unconfined compressive strength conditions.*

### 3.1 Baseline testing series

The complete stress–strain curves of the UCS tests are shown in **Figure 10**. The average values estimated for UCS, CD and CI were 103 MPa, 91 MPa, 39 MPa, respectively for the Jurassic limestone and 125 MPa, 111 MPa and 50 MPa Cobourg limestone.

### 3.2 Relaxation testing series

Two test series have been performed: (i) Jurassic limestone was utilized to examine the applicability of various testing procedures (i.e. axial strain-controlled, radial strain-controlled, multi-step and single-step) for assessing the long-term relaxation behavior and (b) Cobourg limestone was performed utilizing a single-step axial strain-controlled testing procedure.

Emphasis was given to the maximum stress relaxation; the total change between the maximum stress value at the end of loading and before relaxation started. The lowest stress level resulted after relaxation with time. The steps of the procedure undertaken were the following:

- the maximum stress value before relaxation was recorded,
- the initial loading portion of the stress–strain curve was then removed,
- setting the time to zero at the point where the axial strain was kept constant,
- the load rate was kept the same for all the tests, and the initial loading duration ranged from 2 to 20 minutes,
- the axial stress was then normalized to the estimated average UCS,
- the maximum normalized stress was recorded and related to the maximum stress relaxation (the difference between the initial maximum stress and the minimum stress at the end of the relaxation test where no further relaxation took place).

The relations between the maximum stress relaxation and applied stress expressed as a driving ratio of UCS from all the relaxation testing series (axial strain-controlled) are summarized in **Figure 11**. It can be observed that there is an apparent trend between the multi-step and the single-step tests of Jurassic limestone. It can be easily seen that the multi-step tests exhibit less relaxation for similar driving stress-ratios than the single-step. The initial drop in stress mechanism that occurs rapidly for the first step of any test was attributed to being associated with the elastic energy within the sample and load system. A correction procedure was developed since the stress drop was associated with only the initial load stage. This stress drop was added to all subsequent load steps in the multi-step tests, shown (**Figure 11**) as corrected and exhibits similar amounts of stress relaxation compared with the single-step relaxation at a similar load level. Therefore, the multi-step tests, if corrected, can be conducted when limited samples are available [33]. Cobourg limestone shows a higher relaxation sensitivity as it exhibits more stress relaxation than the Jurassic limestone at the same stress levels.

### 3.2.1 Defining the three stages of stress relaxation

All the single-step test results showed a similar behavior during stress relaxation for both the limestones. This behavior can be characterized by three distinct stages, which were observed in the stress relaxation versus time graphs. An example of the test results is illustrated in **Figure 12**. The three stages can also be observed in the radial strain response with time, although there is a slight delay during the transition from stage to stage compared to the transition time of the stress relaxation shown as  $\Delta t$  in **Figures 12** and **13**.

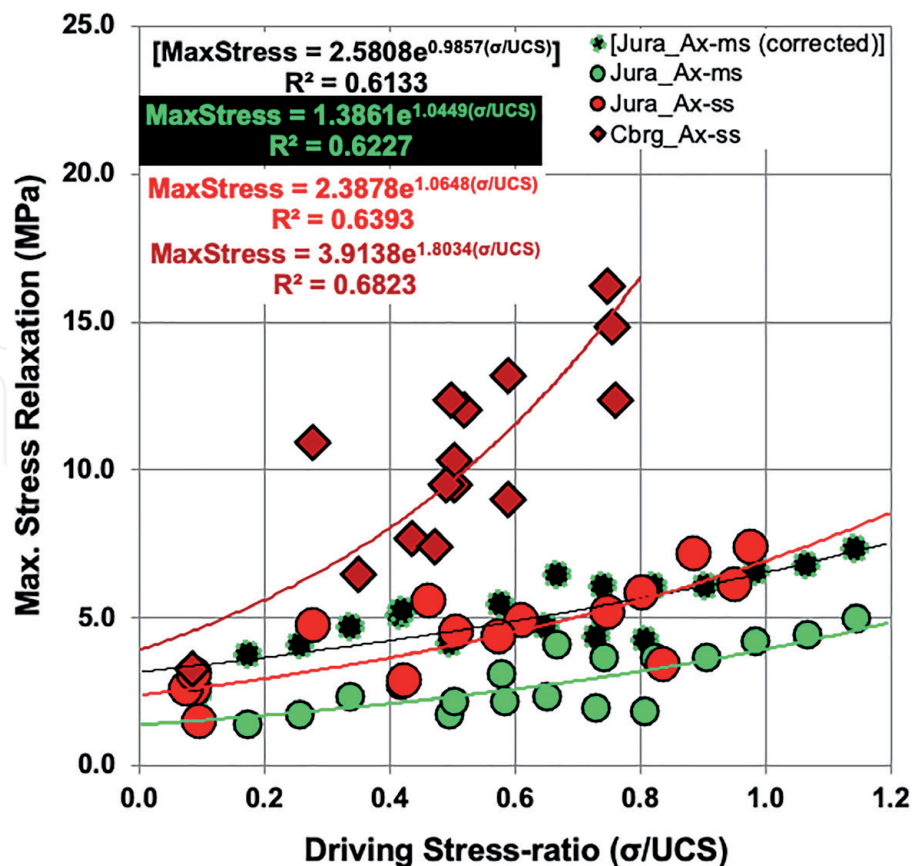


**Figure 11.** Maximum stress–relaxation (MPa) to driving stress-ratio normalized to UCS of the single-step tests on the Jurassic and Cobourg samples, as well as the multi-step tests of the Jurassic samples. ‘Ax’ refers to axial strain-controlled conditions and ‘ss’ and ‘ms’ denotes single-step load and multi-step load tests, respectively.

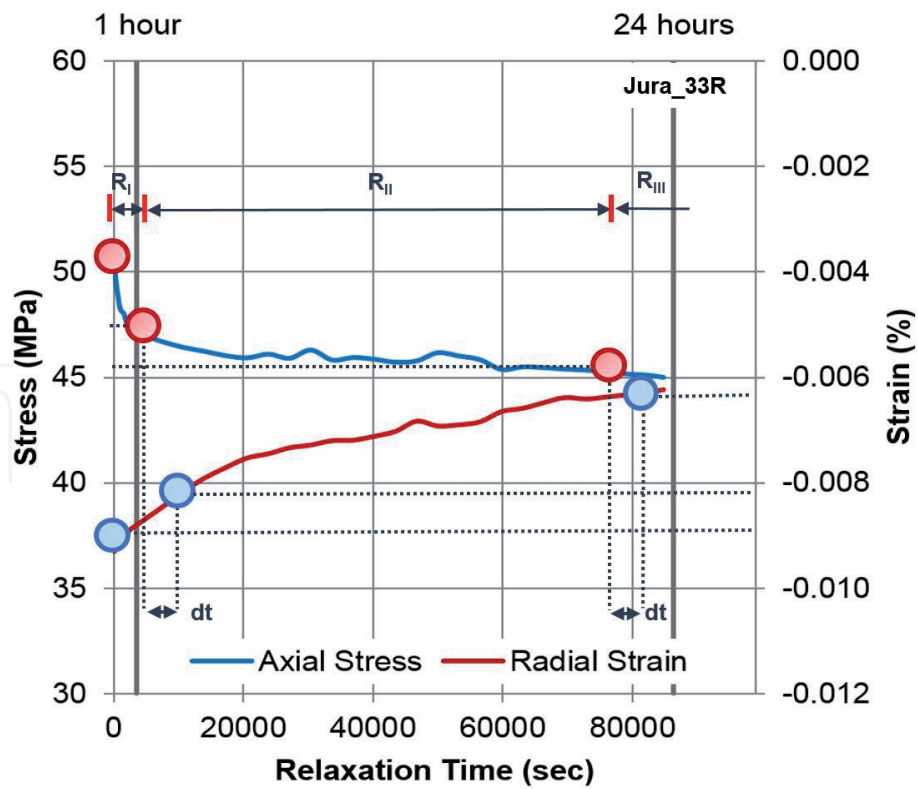


Figure 12.  
The three stages of the stress relaxation process during a relaxation test under axial strain-controlled conditions illustrated on the Jura\_33R sample.

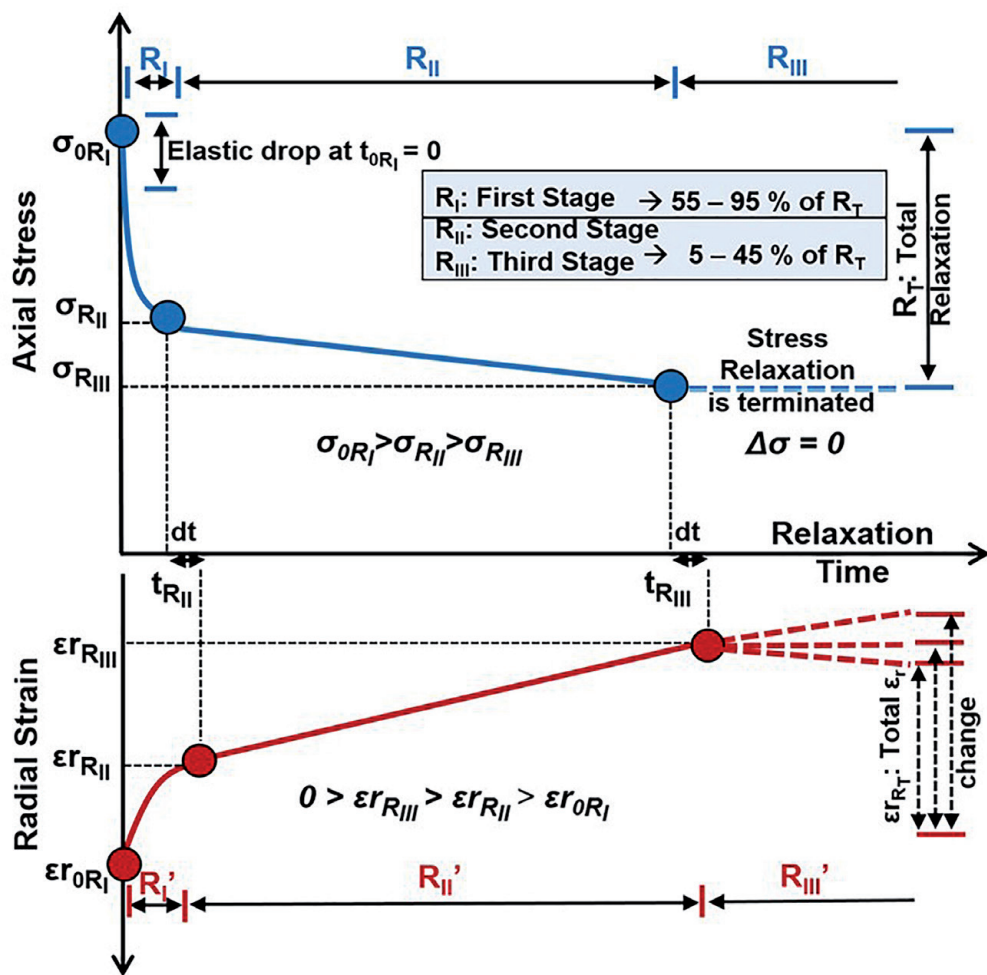


Figure 13.  
The three stages of the stress relaxation process during a relaxation test under axial strain-controlled conditions.

When the axial deformation is kept constant, the stress relaxes at a decreasing rate; this period is defined as the first stage of stress relaxation (RI). At the end of this stage, the stress decrease approaches a constant rate, which marks the second stage transition (RII). The third stage of relaxation (RIII) follows where no further stress relaxation is measurable. At this stage, the stress reaches an asymptote, and the stress relaxation process is effectively complete, which others have observed [19]. Some samples did not exhibit the second stage of relaxation (RII), and in the first stage, 55% to 95% of the total stress relaxation takes place.

The radial strain does not always reach an asymptote. In this case the material is subject to a practically constant axial stress state with ongoing additional absolute radial strain decrease. This response is possibly related to a combination of three-dimensional visco-elastic response and crack behavior during stable propagation (in the axial direction) under constant axial strain.

The significance of this scientific observation should be considered during the excavation of an underground opening. Energy release and stress relaxation in such conditions commonly take place at the face of the excavated tunnel. The created free space disturbs the stress regime of the in-situ conditions. For the stress to re-distribute itself to a new equilibrium state, the rock mass tends to “relax” through the structural geological imperfections (i.e. discontinuities, fractures, joints) of the surrounding rock mass or the newly created fractures due to the excavation method and techniques used. In relation to the scientific observation of the three stages (Figure 14), it would be expected that the rock mass would relax in distinct but possibly overlapping stages. This can serve as an explanation of the sound of cracking closer to the tunnel face without observed failure. Another component of stress relaxation is the duration of this phenomenon until it is terminated. Knowing the duration of stress relaxation can be valuable in the support design and the installation timing, avoiding safety implications arising from support overstepping or resulting in cost savings.

3.3 Static load testing series

Single-step static load tests were conducted on 10 Jurassic, and 4 Cobourg samples and they were held at stress levels above CI for seconds to several days

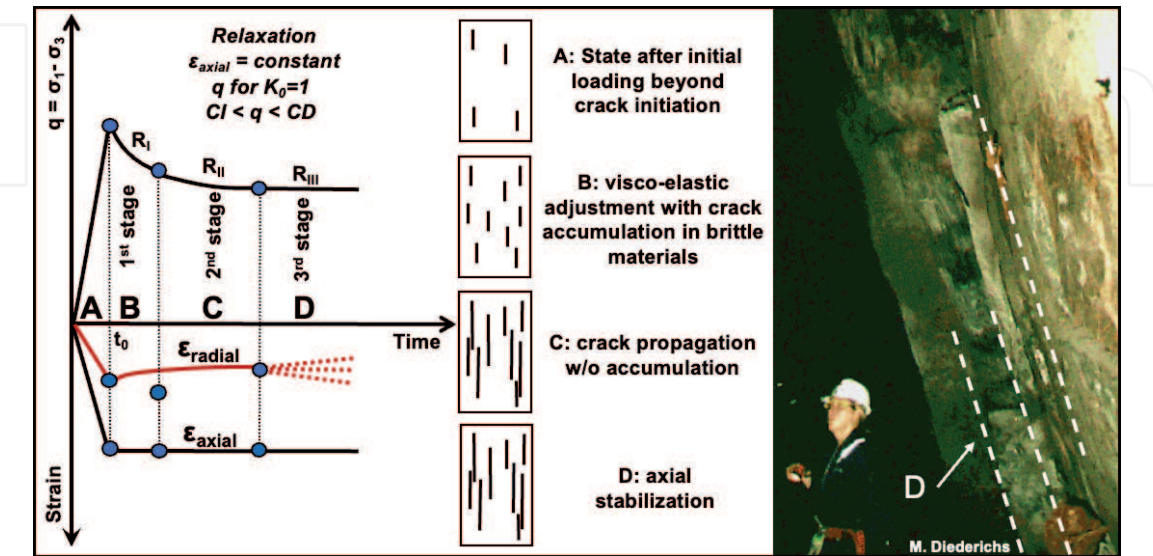


Figure 14. The three stages of the stress relaxation process during a relaxation test under axial-strain–strain-controlled conditions and the response of the material during each stage, dashed lines on the right photo show axial stabilization of damage.

until failure occurred. Most of the single-step tests failed within the first few hours. Several samples did not fail after several days to weeks, at which time the test was terminated. While more practical and convenient, the single-step tests require the testing of more specimens to fully cover the spectrum of the expected range of time to failure. Multi-step tests were performed on three samples, 2 Jurassic and 1 Cobourg, to compare with stress levels derived from the single-step tests. The stress difference between the steps (varying between 2–4) was 5 MPa, and the duration of each step varied from 1 hour up to 10 days until failure took place. A few Jurassic samples did not fail, and it was decided to terminate these tests and unload the samples. To examine the long-term strength and time to failure of a material, the specimens need to fail under a constant load.

The static load testing began at load levels close to the peak strength, based on the Baseline Test results. Subsequent tests were conducted at lower driving stress levels approaching CD and below. In these tests, the constant target stress is applied and maintained by controlling the axial load while measuring the strains (axial and lateral) that increase as the sample proceeds toward failure. Samples loaded close to the peak strength fail catastrophically into many fragments, while samples loaded closer to CD fail less violently. Selected results are presented in this section, serving as examples to describe the main influencing factors during the two limestone tests' creep process.

Two aspects of time-dependency were examined: the first was to derive visco-elastic (creep) parameters for use in the Burgers model (or related models), and the second, the time to failure. Samples that did not fail were also examined to assess the potential reason why some samples fail, and others do not, even at the same driving stress-ratio. For this reason, this section focuses on analyzing and comparing the data from this testing series to other data available in the literature.

However, during the loading phase, the properties of the sample can be determined, such as the stiffness or the damage thresholds. The steps of the analysis procedure were:

- the maximum stress value at which the axial load was held constant was recorded.
- the initial loading portion of the stress–strain curve was used to estimate CI stress thresholds.
- the load rate was similar for all the tests and depending on the instantaneous stress level the initial loading duration ranged from 5 to 10 minutes, according to the ISRM [42] guidelines.
- setting the time to zero at the point where the axial load is kept constant,
- the maximum stress was normalized to an estimated UCS value for comparison to the literature.
- the maximum stress was normalized to the CI value from each sample test, as it is an independent value.
- the visco-elastic parameters were determined.

All the results presented refer to unconfined conditions.

### 3.3.1 Estimating the driving stress-ratio

In the literature, most of the testing results are presented in the form of time against the driving-stress-ratio, defined and used as the stress normalized by the strength of the sample. In most cases, the UCS is taken as an average value from standard UCS tests. In this section, a new solution is presented to examine similar datasets.

[45] suggested that there is a consistent relationship between UCS and CI for brittle rocks. The author has found this to be true for a number of test series with similar lithologies and compatible testing protocols [46]. It was decided to convert the CI values from this study's static load tests to an equivalent UCS value. The CI and UCS values from the Baseline testing series for the two types of limestone were used to develop the conversion factor (here: 2.66 for Jurassic and 2.52 for Cobourg), shown in **Figure 15**. The conversion factors were multiplied with the CI values estimated from the loading portion of the static load test for each sample. [26] suggested that the modified UCS\* can be calculated using Eqs. (3) and (4):

$$UCS^* = a * CI \quad (3)$$

$$a = \frac{UCS^B}{CI^B} \quad (4)$$

where: UCS\* is the estimated UCS, CI is the Crack Initiation value derived from the static load test,  $\alpha$  is a constant and describes the slope of the CI versus UCS graph, and the superscript B denotes values from the Baseline Testing.

When the data (red circles and squares) are compared with other static load test results from various rock types, the time to failure of the samples from this

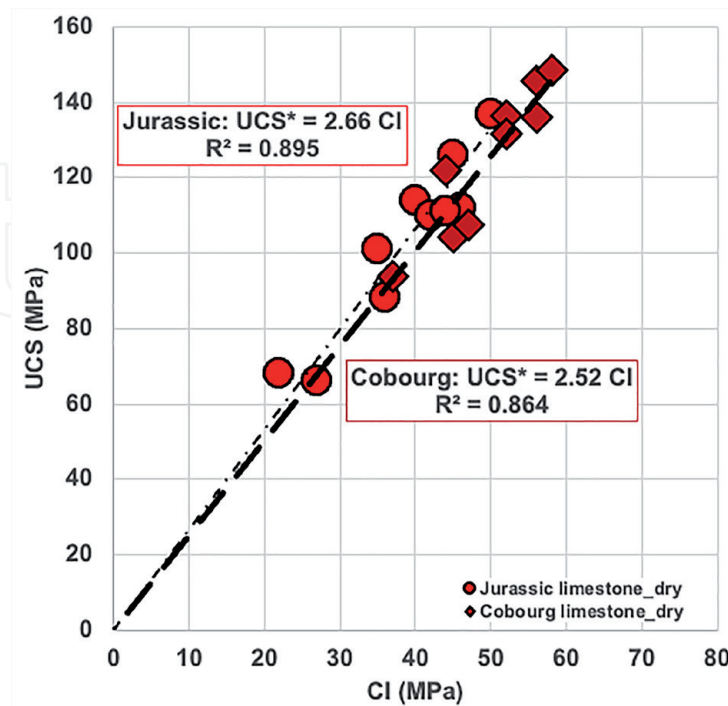


**Figure 15.**

*The relationship between UCS and CI for the Jurassic and Cobourg limestone from the baseline testing.*

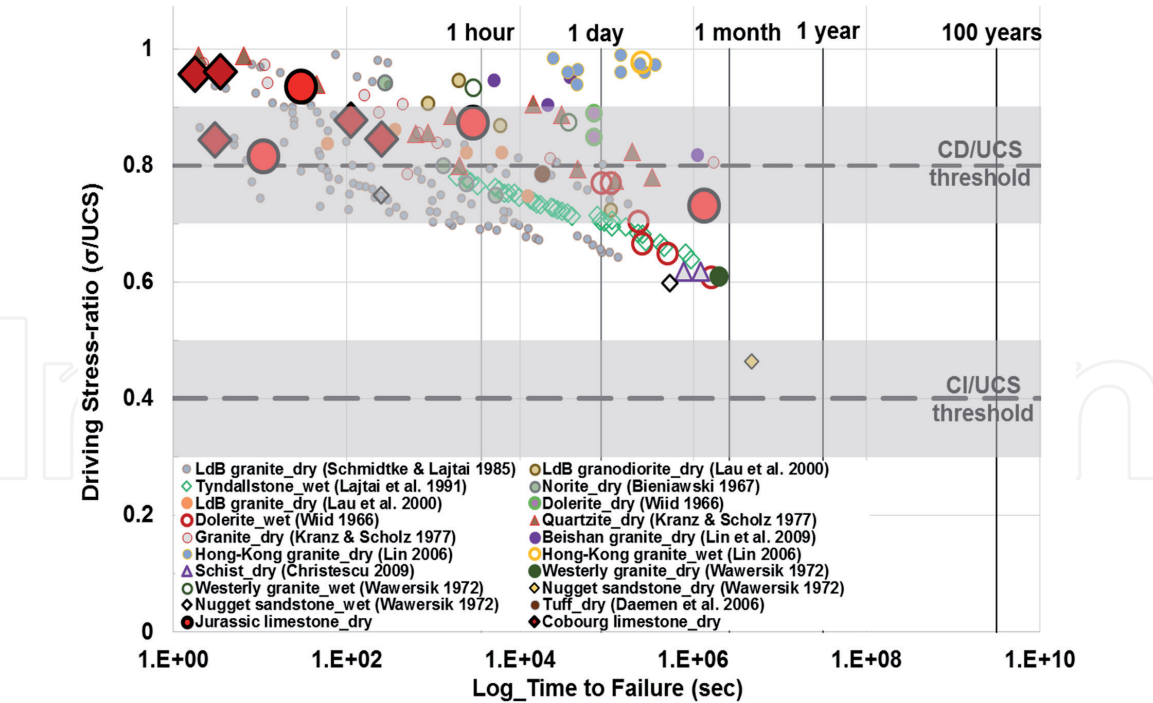


**Figure 16.**  
Static load test data for hard rocks performed at room temperature in wet or dry conditions (where the driving stress-ratio is the stress level at failure to unconfined compressive strength of the material).

study seems to follow a similar trend (**Figure 16**). There are no samples loaded below the CI threshold that fail from the data presented and gathered from the literature.

**Figure 17** categorizes the data according to the main rock type, sedimentary, metamorphic, and igneous.

The sedimentary rocks appear to follow a similar trend with the metamorphic rocks. In contrast, igneous rocks show more scatter because most test results have been on igneous rocks and that there are fewer results on sedimentary and metamorphic. There could also be due to different grain sizes of the granitic rocks tested characterized by grain-scale heterogeneity.

Granites and limestones, even though they fail similarly following brittle failure theory principles, their long-term strength is directly dependent on lithology, as better shown in **Figure 18**. Due to heterogeneous mineralogy and their different intrinsic properties, granitic rocks allow other creep behavior within different constituent crystal grains. Steady creep creates mechanical conflicts between the different grains and damage results. This creep-induced damage process is less dominant in monomineralic limestones, and therefore creep can occur with less resultant weakening.

Differences in the trend start to emerge when examining individual sample sets. The latter is partly because there is a lack of statistically representative data sets on an individual sample set, except the lac du bonnet set.

From **Figure 19**, it is evident that above 0.8 ucs or the cd threshold, all samples failed within an hour. Below the ci threshold, where pre-existing cracks are closing, and elastic strains govern, no failure should occur as [47, 48] reported from testing cobourg limestone samples for up to 100 days. Commonly, the static load stress levels fall between the ci and the cd thresholds. This region is an uncertain region since between ci and cd crack propagation, and accumulation of damage occurs in the short-term. Still, in the long-term, the time component can degrade the rock,

further leading it to failure. However, below 0.7 ucs, no failure is shown. These no-failure points could be the result of not holding the load constant for long enough. Data from the literature suggests that failure could be expected at such driving stress-ratios. Tests from 6 months to 1 year are advised to examine if samples of the limestones in this study would fail at such driving stress-ratios over the long-term. The time-dependent behavior discussed in this section is interpreted to be, in part, the result of the behavior of new microcracks, the intensity of which impacts the final ucs value [49].

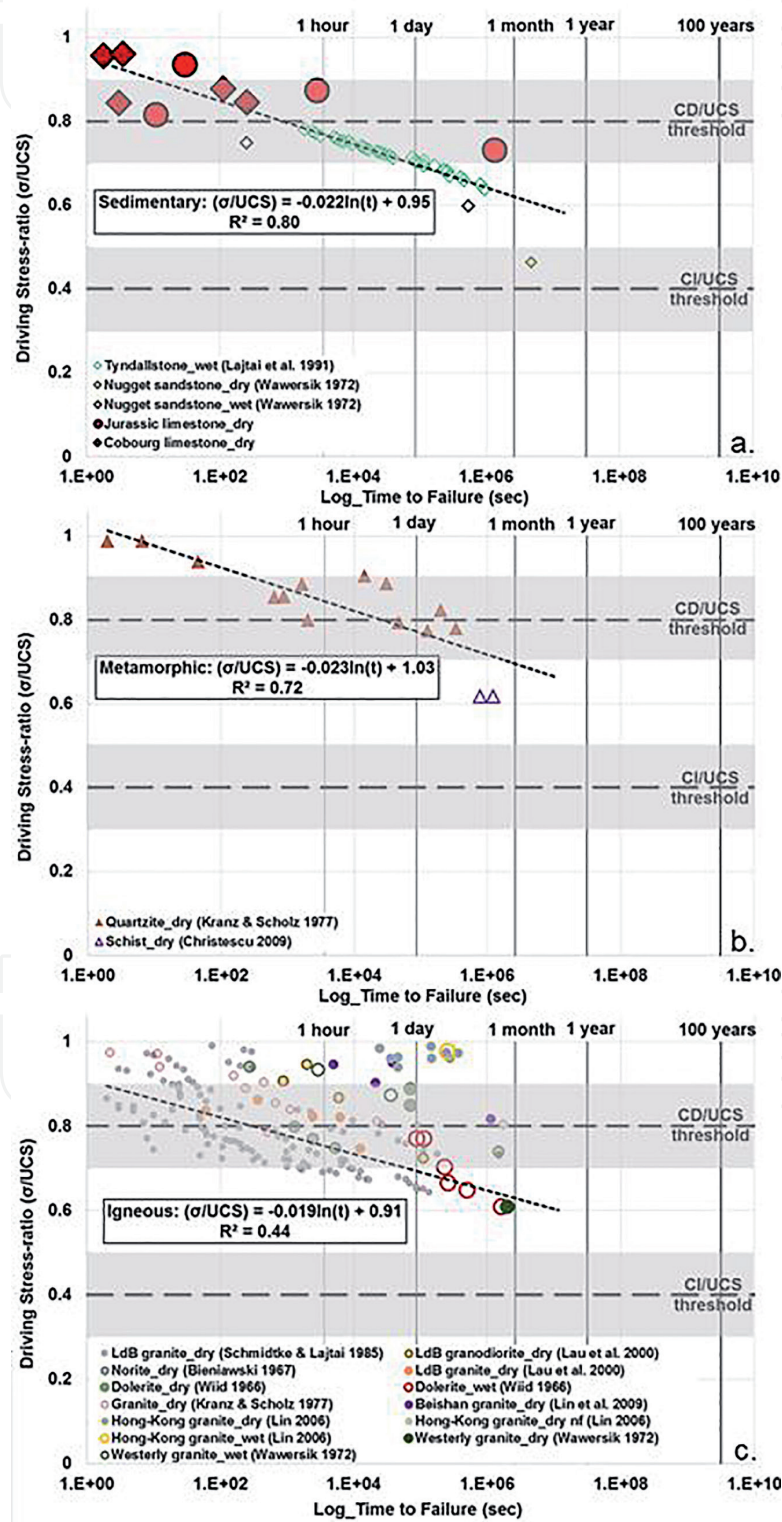


**Figure 17.** Static load test data for: (a) sedimentary, (b) metamorphic, (c) igneous rocks performed at room temperature in wet or dry conditions (where the driving stress-ratio is the stress level at failure to unconfined compressive strength of the material).

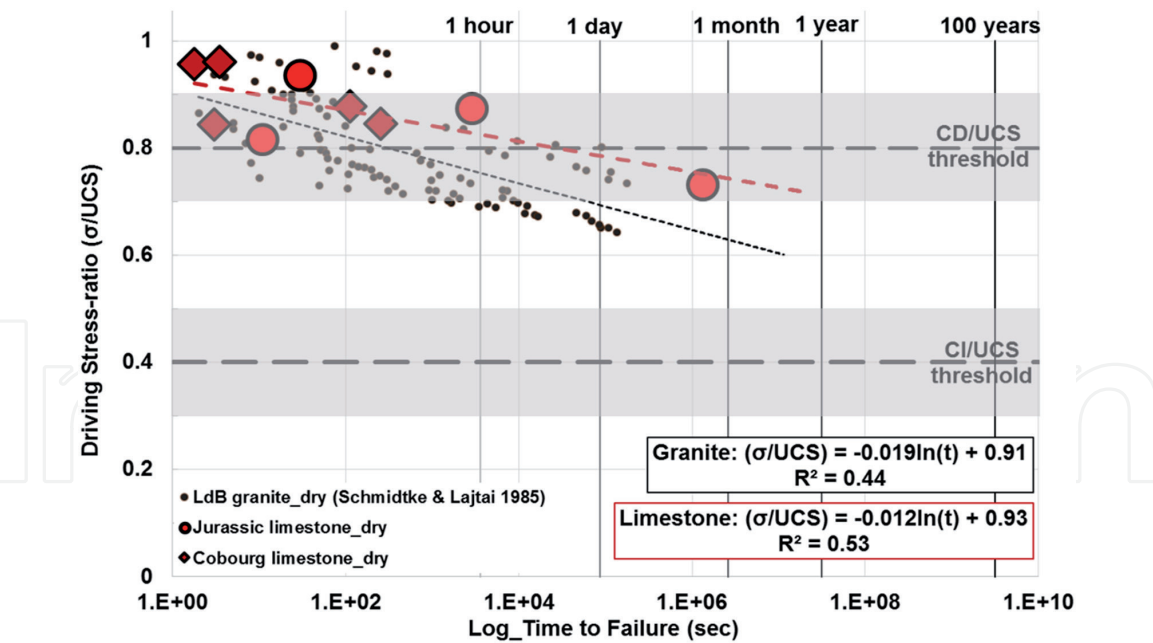


Figure 18.  
comparison of static load test data on limestone and granite performed at room temperature in dry conditions (where the driving stress-ratio is the stress level at failure to unconfined compressive strength of the material).

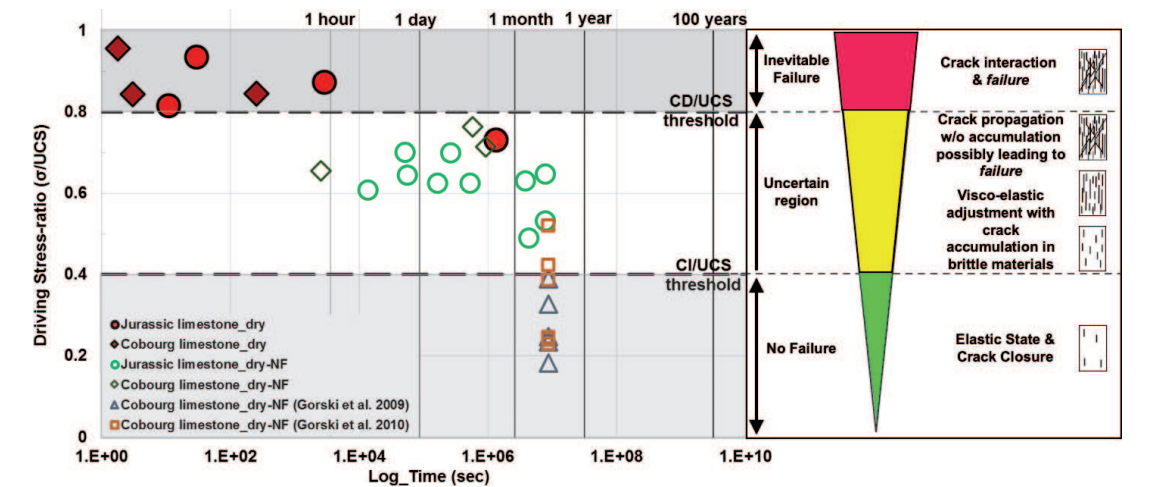


Figure 19.  
static load test data of jurassic and cobourg limestone performed at room temperature in dry conditions (where the driving stress-ratio is the stress level at failure to unconfined compressive strength of the material). The 'nf' in the legend indicates samples or tests did not fail whereas the 'f' denotes samples or tests reach failure.

## 4. Time-dependent effects in tunneling

Time-dependent deformations associated with rock tunneling are a reality that warrants further investigation and understanding and can be observed during excavation and/or after the construction period of the project.

### 4.1 Analysis of time-dependent rock masses using the convergence-confinement method

Understanding the nature and origin of deformations due to an underground opening requires, as [50] noted, both knowledge of the rock-support interaction and field data interpretation. This tunnel wall movement, also known as convergence, results from both the tunnel face advancement and the time-dependent behavior of the rock mass.

The Convergence-Confinement Method (CCM) is a two-dimensional simplified approach that can be used to simulate three-dimensional problems. Analytical solutions based on CCM (usually examine either the effect of tunnel advancement or the time-effect) could be partially used to select the final support. One may wonder if it could also be possible to simulate and replicate the complete problem. Time-dependency is acting during the timeframe of construction impacts, the so-called Longitudinal Displacement Profiles (LDPs) for deformation estimation during tunnel advance. LDP is an accompanying tool used with the Ground Reaction Curves (GRC) used in the CCM to relate internal wall pressure relaxation to tunnel displacement. Suggested analytical solutions for LDPs [50], etc.) refer to elastic or elasto-plastic rock materials. **Figure 20** schematically illustrates the effect of both time and tunnel advancement on the LDP of a tunnel excavated in a visco-elastic medium. The tunnel's advance is simulated by reducing the internal pressure,  $p_i$ , initially acting on the tunnel core (as  $p_0$ ). The rock responds by convergent deformations (via the GRC), which are, in turn, linked to the tunnel advance via the LDP. This aspect of time-dependency is also discussed, examined and further analyzed in this chapter.

Analytical and closed-form solutions that consider the time-dependent convergence have been proposed in the literature for supported and unsupported tunnels with linear and non-linear visco-elastic medium [51, 52], etc. Most of these formulations also consider the tunnel advance in the estimated total deformation yet are found to be impractical due to the complex calculations required [53, 54].

**Figure 21** illustrates the anticipated LDP of the tunnel displacement in an elasto-visco-elastic medium where no tertiary creep takes place. More ductile materials, as in the case of rock salt, can behave in such a manner. It is shown that when no time-effect is considered, the total displacements are underestimated, which can lead to erroneous calculations at the initial stages of the design process.

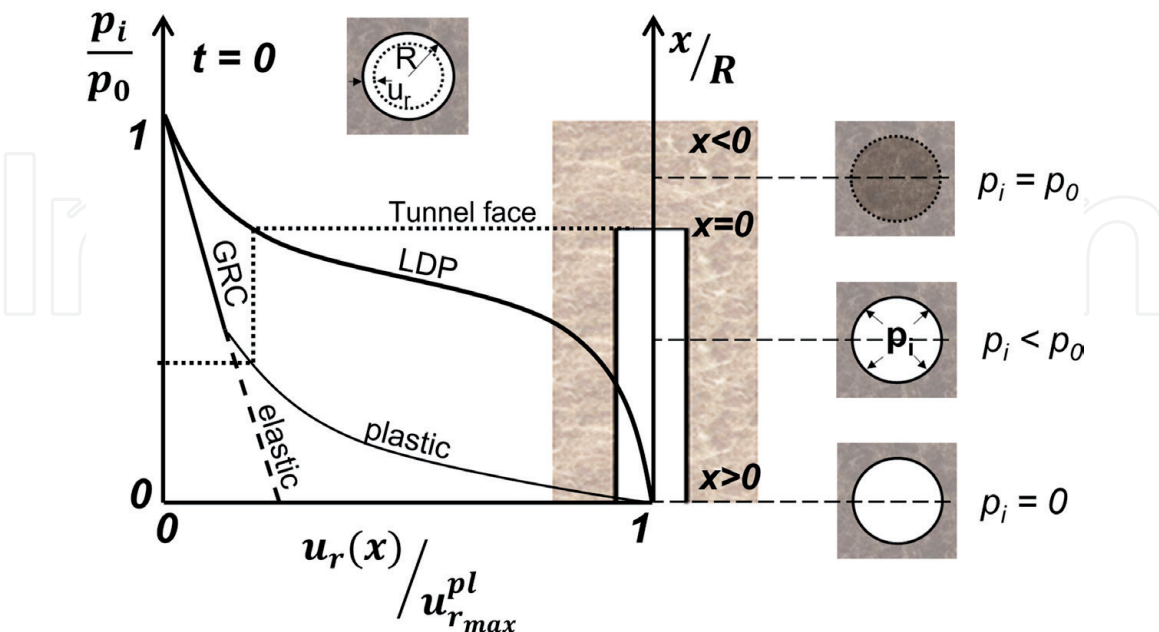


**Figure 20.**

Schematic representation of the GRC of an elastic ( $t = 0$ ) and a visco-elastic material ( $t > 0$ ) and their relation to the LDP. Y-axis on the left refers to the internal pressure ( $p_i$ ) normalized to the in-situ pressure ( $p_0$ ), Y-axis on the right refers to the distance from the face ( $x$ ) normalized to the tunnel radius ( $R$ ) and X-axis refers to the radial displacement at a location  $x$  normalized to the maximum radial displacement due where  $t$  denotes time and subscripts  $e$  and  $ve$  refer to elastic and visco-elastic material, respectively.

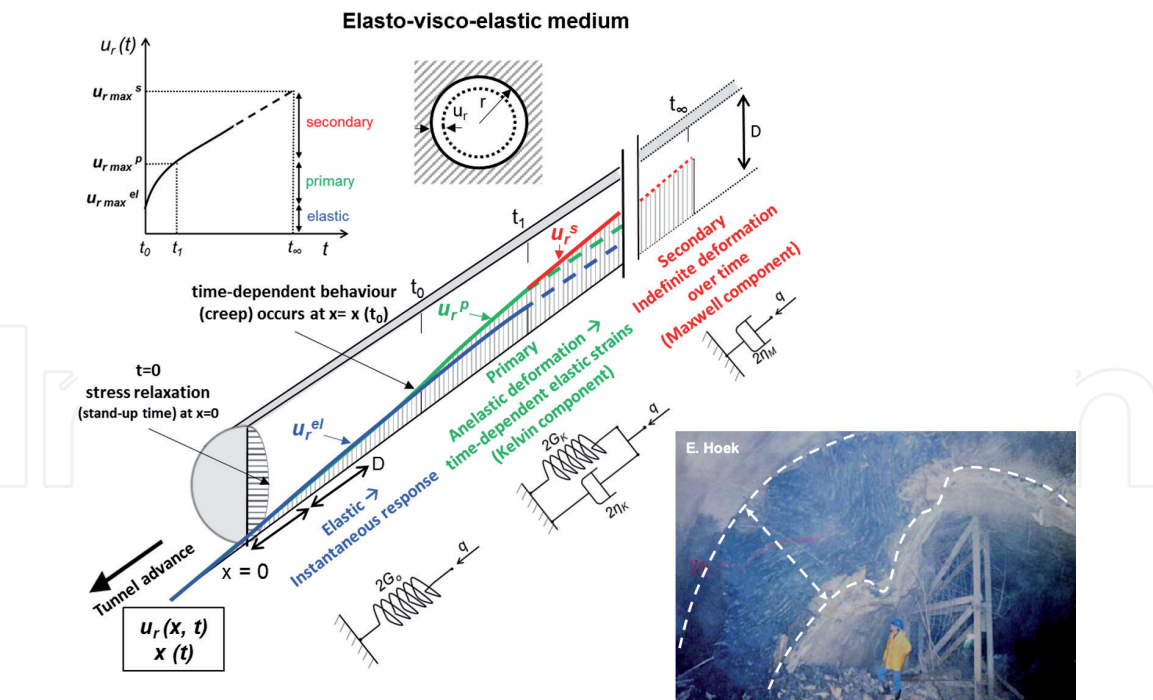


**Figure 21.**  
Schematic representation of the longitudinal displacement profile (LDP) in an elasto-visco-elastic medium.

4.2 Capturing the time-effect in tunneling using a new numerical approach

An axisymmetric parametric analysis was performed within FLAC software. The geometry of the model and the excavation sequence characteristics are shown in **Figure 22**. A circular tunnel of 6 m diameter and 400 m length was excavated in isotropic conditions. Full-face excavation was adopted. Two cases of a drill and blast (Case 1: D&B) and a TBM (Case 2: TBM) were assumed depending on the excavation step 1 m and 3 m, respectively. The rock mass was set to behave as an elasto-visco-elastic material using the CVISC model. The analysis aimed to examine the contribution of primary and secondary creep. In this regard, the Maxwell body’s viscous dashpots within the CVISC model were deactivated and reactivated,

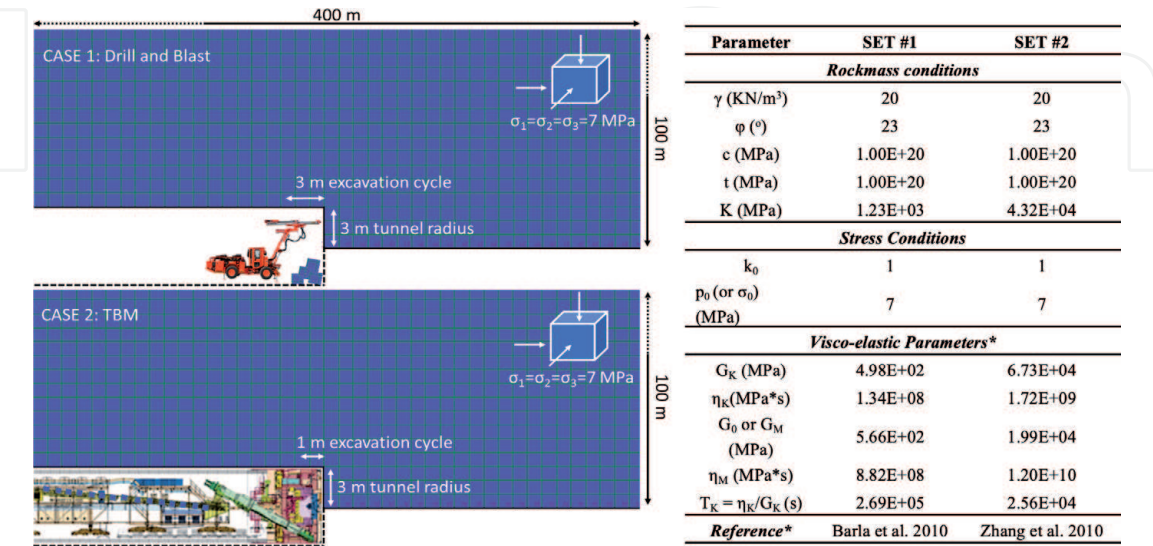


**Figure 22.**  
(Left) Schematic illustration of the excavation sequence used within the numerical axisymmetric analysis; case 1 refers to drill and blast method with 3 m excavation step per cycle; case 2 refers to TBM (Tunneling boring machine) method with 1 m excavation per cycle. (Right) Parameters used for CVISC model.

accordingly. Besides, two different sets of visco-elastic (creep) parameters were used then for both cases shown in **Figure 22**. Furthermore, the excavation cycle duration was also simulated to consider both the time-dependent component and the tunnel advance representing the real conditions in a tunnel problem and varied from 2 to 8 hours. In addition, two supplementary analyses were performed: with the Kelvin-Voigt model and with the elastic model to validate the numerical models and compared with analytical solutions.

It should be stated that the visco-elastic parameters were chosen according to the analytical solution (Eq. (5)) of the Kelvin-Voigt model developed by [51].

$$u_r = \frac{\sigma_o r}{2G_o} + \frac{\sigma_o r}{2G_K} \left[ 1 - \exp\left(-\frac{t}{T_K}\right) \right] \quad (5)$$

(where:  $\sigma_o$  is the in-situ stress conditions,  $r$  is the tunnel radius,  $G_o$  the elastic shear modulus,  $G_K$  is the Kelvin shear Modulus,  $\eta_K$  is Kelvin's viscosity and  $T_K$  is known as retardation time and it is the ratio of Kelvin's viscosity over the Kelvin Shear Modulus and is indicator of when the model will convergence and reach a constant value.)

The selected retardation time ( $T_K$ ) varies one order of magnitude between the two sets as it controls the curvature of Kelvin's model behavior. The following **Figures 24** and **25** 'x' is the distance from the tunnel face,  $R$  is the tunnel radius,  $u_r$  is the absolute radial tunnel wall displacement,  $u_{r,max}$  is the maximum elastic displacement and  $u_{r,\infty,max}$  is the maximum visco-elastic displacement of the Kelvin-Voigt model. Gray and black lines are the elastic and the zero-viscosity KV models respectively.

#### 4.2.1 Primary stage of creep, KELVIN-VOIGT (KV)

The Kelvin-Voigt model was assumed to represent the primary stage of creep and was used to simulate an elasto-visco-elastic rock mass's mechanical behavior. The results for both cases are presented in **Figure 23**. They imply that increased cycle time or excavation delay exacerbates the rock mass's mechanical behavior; as in all models, an increase of the ultimate total displacement was observed. This increase depends on the visco-elastic parameters of the Kelvin-Voigt model. The increase of the retardation time will increase the time required by the model to reach a constant value and become time-independent.

The deviatoric stress was related to the displacement data normalized to the maximum displacement of the Kelvin-Voigt model ( $u_{r,\infty,max}$ ). Time-dependent behavior starts for both cases when the deviatoric stress reaches a critical value ( $q_{cr}$ ) shown in **Figure 23b**. This critical value is attained after one excavation step at the point which the time-dependent LDPs deviate from the elastic LDP. In the drill and blast case, this is 3 m away from the tunnel, whereas for the TBM case it is 1 m.

#### 4.2.2 Secondary stage of creep, Burgers (B)

The second stage of this analysis was to investigate the influence of both primary and secondary creep behavior stages using the Burgers model. The results presented in **Figure 24** show the maximum strains due to the secondary stage (Maxwell) are effectively infinite. This is also observed on **Figure 21**. In this part, it was noticed that the magnitude of the total displacements between the two cases varied significantly. The excavation method influences the accumulated displacements.

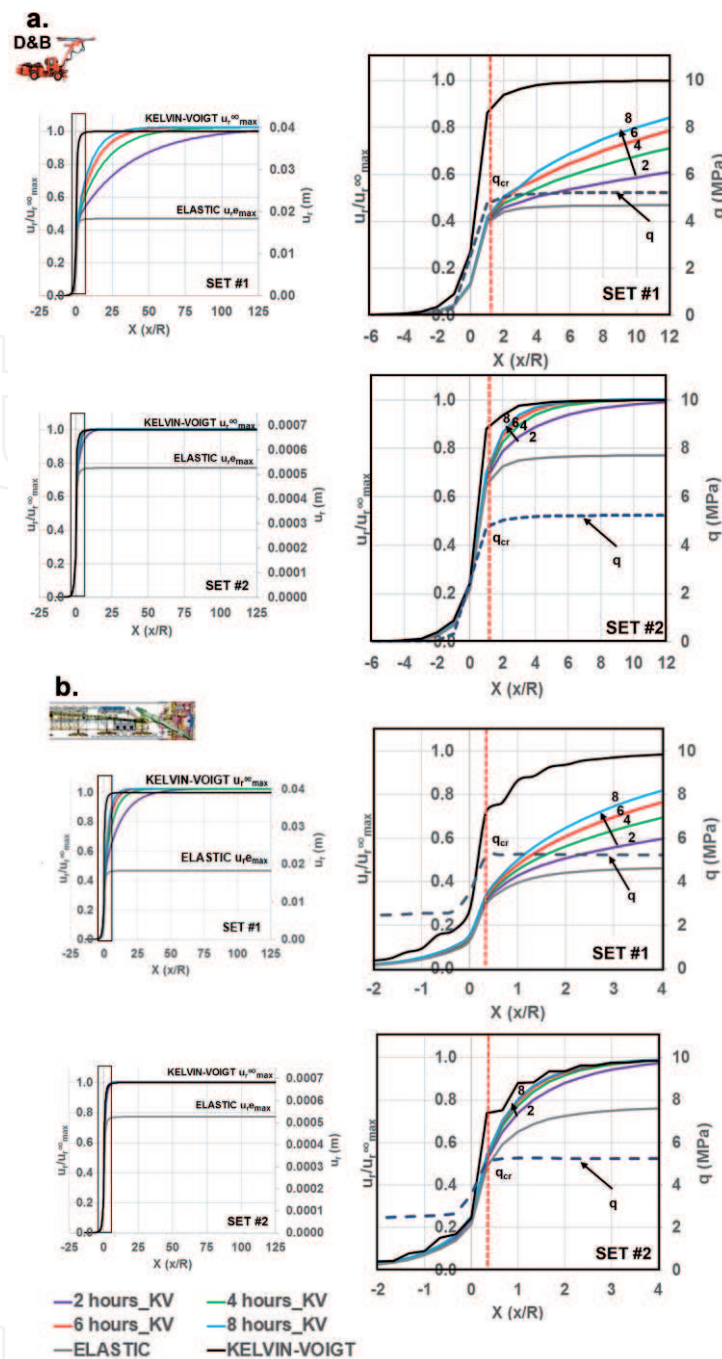


**Figure 23.**  
(Left) Numerical results of LDPs, (right) closer representation of the data; relating the deviatoric stress ( $q$ ) to the tunnel wall displacement normalized to the maximum displacement of the KELVIN-VOIGT model ( $u_{r\infty\max}$ ) for: (a) the drill and blast case (DB) and (b) the TBM case.

In the drill and blast case, all two sets of parameters exhibited less displacement than the TBM case for the same duration of the excavation cycles. During a TBM tunnel excavation, the tunnel excavation requires more time than a drill and blast excavation for the same excavation cycle. For instance, a TBM that excavates 1 m every 6 hours, the elapsed time is three times longer than the drill and blast case of 3 m excavation per cycle. In the TBM case, the time for the excavation of the same length tunnel will result in an accumulation of displacement increase. However, this may not always represent real conditions as TBMs are commonly preferable since they tend to achieve better excavation rates; if proven affordable. Suppose the latter is the case, then a TBM excavation of a two-hour excavation cycle. In that case, it is shown that the surrounding rock mass represented by SET#1 exhibits less displacement than an eight-hour excavation cycle using drill and blast.

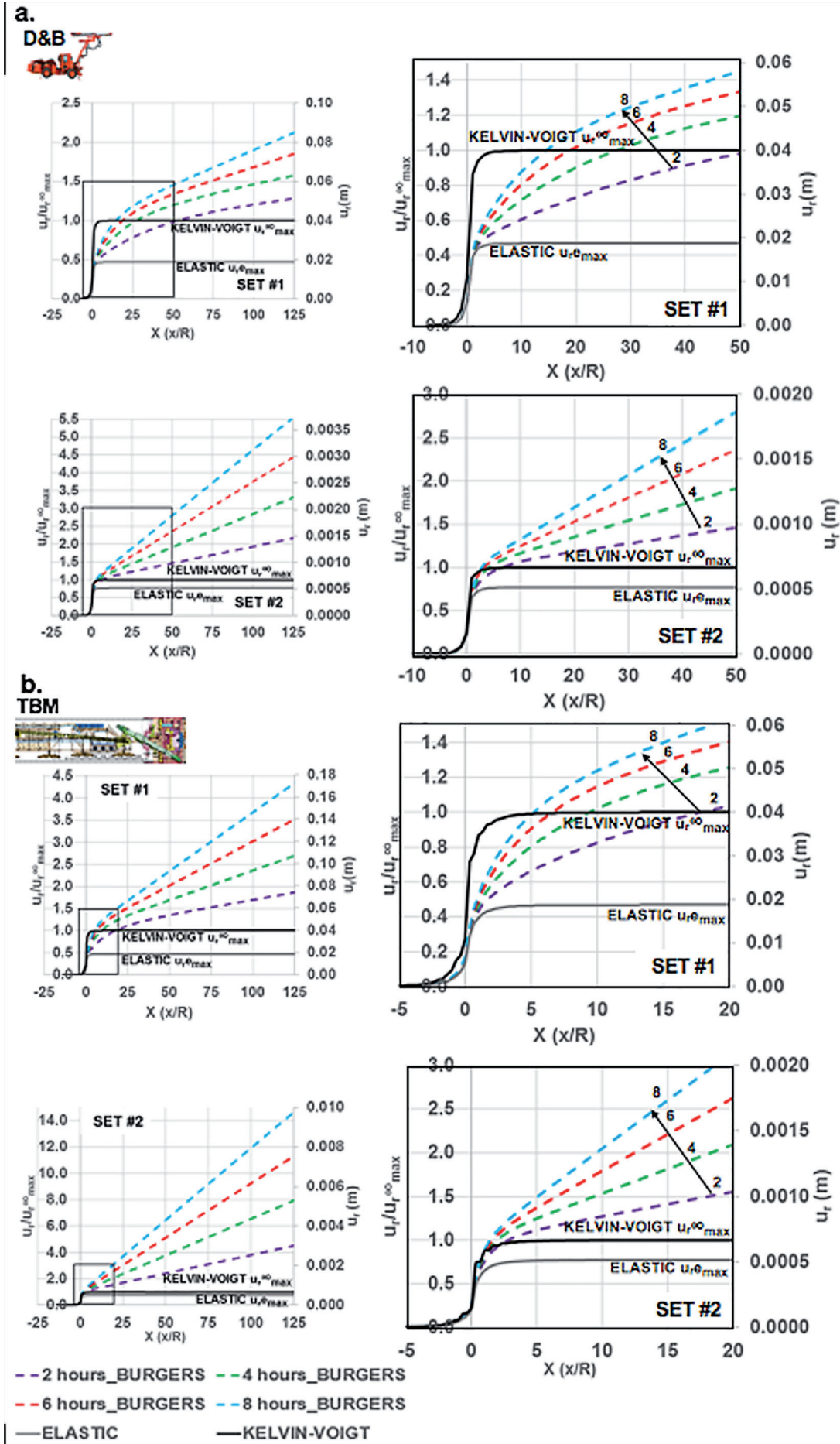


**Figure 24.** (Left) Numerical results of LDPs for: (a) the drill and blast (DB) and (b) the TBM case of the BURGERS (B) analysis (the hours on the legend denote hours per excavation cycle), (right) closer representation of the data.

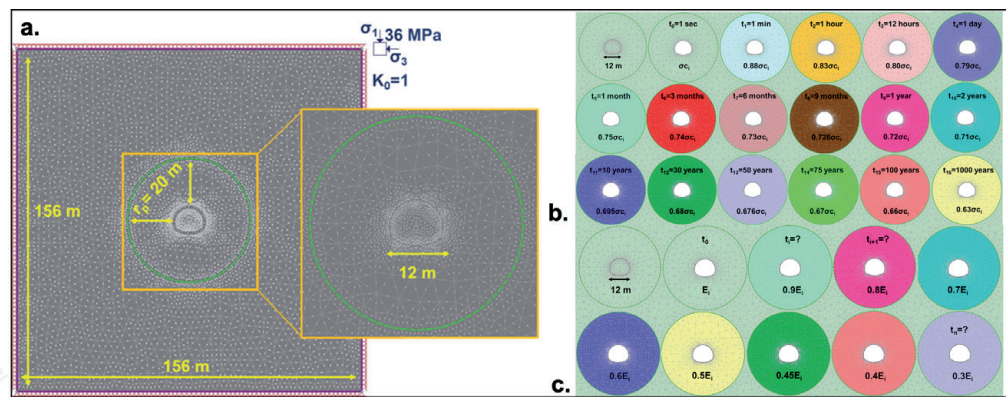


**Figure 25.**  
(a) Geometry and mesh conditions of the model used,  $r_p$  denotes the radius of the plastic zone, and incremental reduction of (b) intact rock strength according to long-term strength and (c) Young's modulus.

### 4.3 Predicting the long-term behavior of rock masses in tunneling

Although there are time-dependent models available to predict rock materials' rheological behavior potential, it is commonly observed that in two-dimension (2D) modeling, time-dependent behavior is not directly simulated using selected 2D coded software with noted limitations [1]. It is, therefore, necessary a method to be developed and 'pseudo' simulate this type of behavior. For instance, the plastic zone can be used as an indicator of the overall time-dependent displacements and calibrated to in-situ measurements or laboratory testing [1].

[25] proposed a new methodology for predicting rock masses' long-term behavior using the information derived when testing rock materials under constant loading, which results in strength degradation by 'pseudo-simulating' numerically this behavior. [25] examined two main sets of numerical models in plane strain conditions in-plane RS2 (Rocscience). The models' main difference was that the material included in the plastic zone changed parameters with time-steps in the one set of models. The first aimed at pseudo-simulating time-dependent behavior by using the Long-Term Strength (LST) according to strength-degradation Eq. (6) of the limestone bases on the laboratory data previously shown in **Figure 18**.

$$(\sigma/\text{UCS}) = -0.022\ln(t) + 0.95 \quad (6)$$

In addition, 19 stages were simulated, as shown in **Figure 25a**. Where in each stage, a new  $\sigma_{ci}$  (strength of intact rock) was assigned only to the material of the plastic zone, according to Eq. (6). Each strength reduction represented a specific time from 1 second to 1000 years. The second set of analyses were based on Young's modulus ( $E_i$ ) reduction from the initial 40 GPa to 12 MPa of 10% in every modeling stage (**Figure 25b**). It should be highlighted that the decrease in both strength and Young's Modulus reduction was applied to the plastic zone, assuming that the rest model behaves as an elastic material.

Every increment on the strength-degradation models was related to a time according to the lab results and time to failure graph shown in **Figure 18**, such as the YMR models can be associated with a specific time. For instance, a reduction of the intact strength of 21% ( $0.79 \sigma_{ci}$ ) can simulate the deformation acquired in 1 day and reflects the deformation of the 30% reduction of Young's Modulus (**Figure 26**). Moreover, to simulate the rock mass's deformation around the tunnel after a 2-year period, one can either reduce the intact strength to  $0.71 \sigma_{ci}$  or reduce the Young's Modulus to 50% (**Figure 26**).

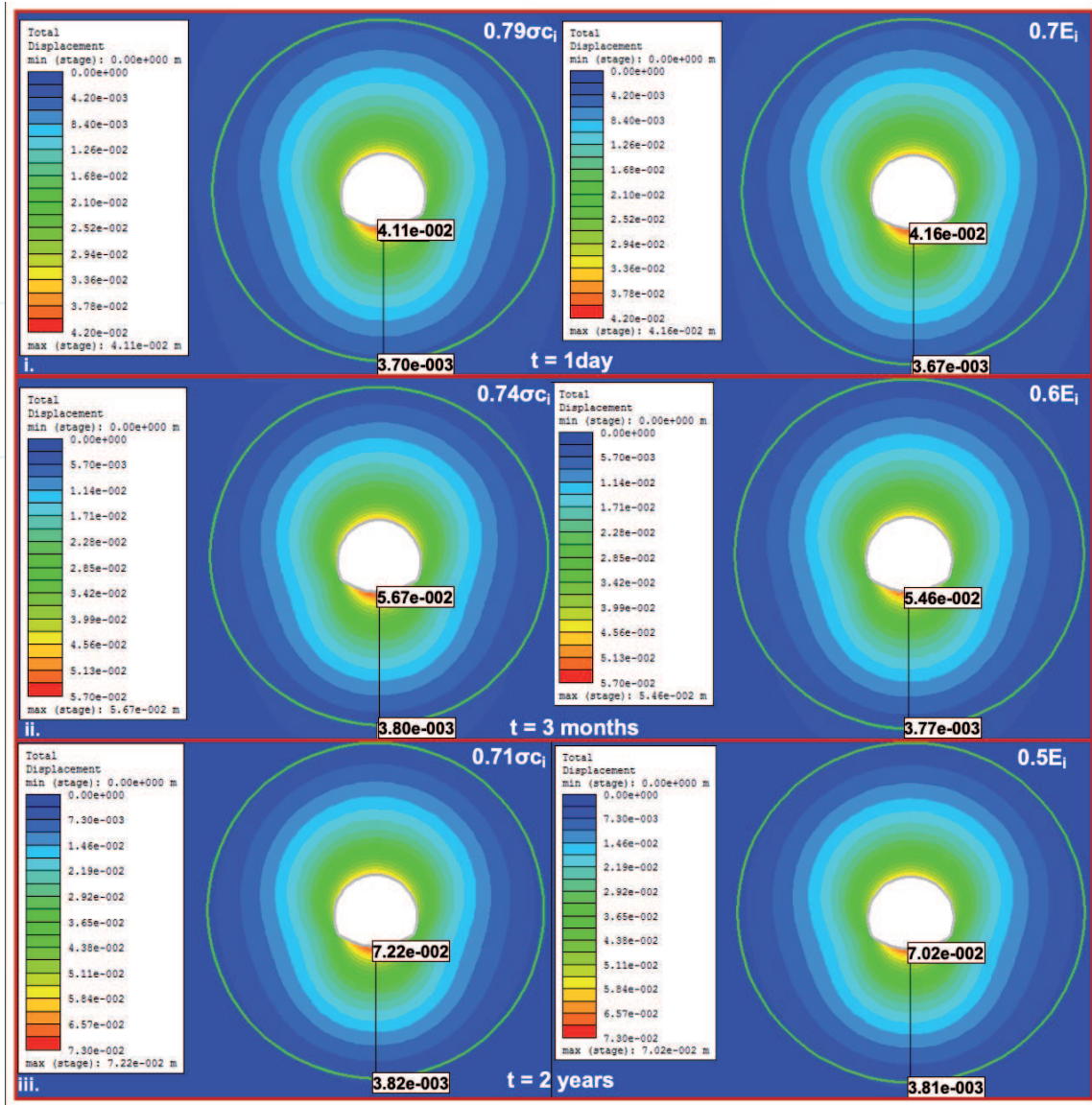


**Figure 26.**  
*Numerical results of total displacements of LST models (left column) and YMR (right column).*

Relating the strength-degradation (or the LTS) with the YMR to time for specific lithologies can produce a database that one can use to capture the time effect on the rock mass behavior, as shown in **Figure 27a**. The yellow triangles reflect the YMR with the time, whereas the green circles the limestone's overall behavior based on the laboratory data (blue and light blue diamonds and squares). When the YMR method is used, the reduction factor can be estimated using Eq. (7), where  $t$  is time, and  $E/E_i$  is Young's Modulus-ratio.

$$\text{YMS of limestone: } (E / E_i) = -0.028 \ln(t) + 1.014 \quad (7)$$

Using this YMR approach proposed by [25] for the granite (**Figure 27b**) the estimated reduction of the Young's Modulus is given in Eq. (8).

$$\text{YMS of granite: } (E / E_i) = -0.03 \ln(t) + 1.018 \quad (8)$$

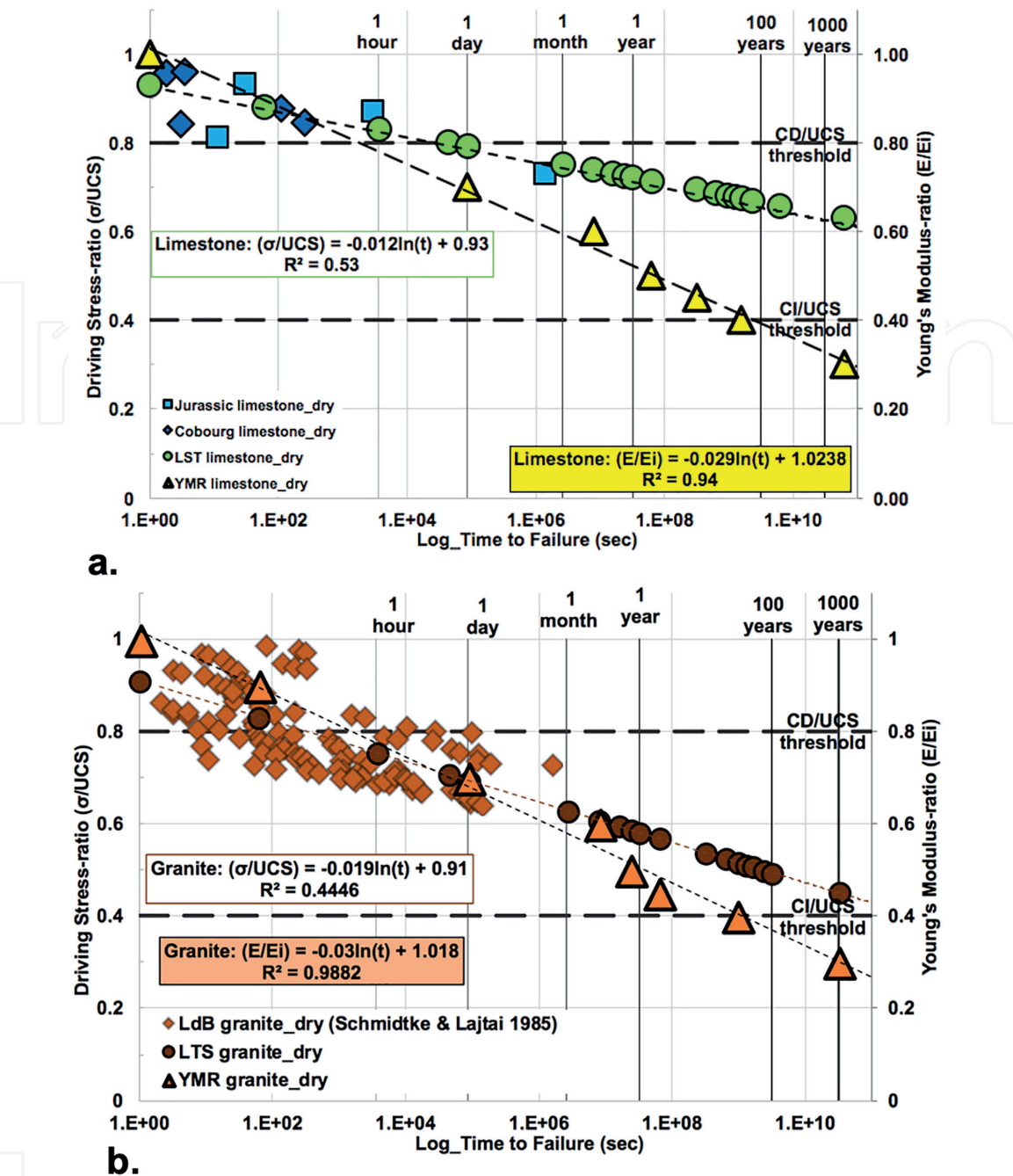


**Figure 27.** Driving stress-ratio and Young's modulus-ratio in relation to time to failure from static load test data performed at room temperature in dry conditions, (where the driving stress-ratio is the stress level at failure to unconfined compressive strength of the material), for a. limestone and b. granite.

It should be stated that the analyses presented herein can be used for values of at least  $0.5\sigma_{ci}$  and higher as the below this threshold (CI), no failure is anticipated, below this threshold, the observed behavior is considered to be linear elastic.

## 5. Conclusions

This research work and the resultant publications presented in this Chapter have contributed to a better understanding of the "Time-dependent behaviour of rock materials". This section summarizes the key findings of this study.

It is widely accepted that significant research contributes to studying the time-dependent behavior of geo-materials and their effects in geoengineering applications by developing models. However, these models mainly focus on simulating the visco-elastic creep behavior and are developed based on the back-analysis of existing datasets. In many cases, these models can replicate sufficiently creep behavior during the primary and secondary stage when appropriate parameters are derived and used. Furthermore, the applicability of such models is commonly broader when dealing with weak rock masses. As a result, there is a knowledge gap when dealing with time-dependent behavior in brittle rock materials. Its effect is considered limited and usually neglected and covered by other progressive damage mechanisms. Nevertheless, this study has shown the importance of taking into consideration brittle time-dependent behavior, and it is recommended that engineers, scientists and practitioners utilize the existing models to simulate time-dependent behavior with appropriate parameters as with a few modifications, these models can capture the behavioral trend as long as the appropriate parameters are utilized.

In this study relaxation, the decrease of applied load at constant deformation was investigated and re-defined. It was shown that relaxation could be considered as an inversion of a creep behavior. It was concluded herein that axial strain-controlled tests are less sensitive to testing challenges during a relaxation test than a creep test. Single-step and multi-step tests have been performed in this study. It was shown that single-step is easier to perform, but there is sample consuming in order to obtain a complete dataset to cover the total stress spectrum. From the results, it was also shown that relaxation takes places when cracks initiate and propagate during the sample. It attains a constant value (asymptote) when axial crack stabilization is reached. The most important outcome of this work was identifying the existence of three distinct stages that occur during time-dependent stress relaxation. These three stages ( $R_I$ ,  $R_{II}$ , and  $R_{III}$ ) were introduced and clearly defined. The first two stages are similar to the first two stages in creep behavior. In contrast, the third stage differs as the sample reaches a stable condition compared to tertiary creep where it reaches failure.

Another set of tests, static load, both single-step and multi-step, are presented here. This time the axial load (stress) was kept constant, focusing on time-dependent behavior over time. Once again, it is shown that multi-step tests might be advantageous in terms of deriving visco-elastic parameters in different target stress levels using only one specimen; however, when considering time-to-failure single-step tests are preferred. In this section, two types of limestone (Jurassic and Cobourg) were investigated, and the time-to-failure behavior was compared to other rock types from data published in the literature. It was concluded that an overall trend does exist. This general trend was scrutinized at a second stage based on rock types providing specific trends for sedimentary, metamorphic, igneous, which can be used to predict time-to-failure for laboratory samples:

- Sedimentary:  $(\sigma/UCS) = -0.022\ln(t) + 0.95$
- Metamorphic:  $(\sigma/UCS) = -0.023\ln(t) + 1.03$
- Igneous:  $(\sigma/UCS) = -0.019\ln(t) + 0.91$

where  $\sigma/UCS$  is the driving stress-ratation and  $t$  refers to time.

The limestone dataset was compared to the widely used dataset of Lac du Bonnet granite, showing that the limestone's long-term strength is higher than the granite. The latter means that the limestone can withstand longer time-depended behavior than the granite. The latter can be explained by the fact that these two rock types

differ in their mineralogical structures. The granite's increased heterogeneity contributes to different creep rates of the various grains (quartz, feldspars, mica). The latter generates incompatible strains over time, causing micro-cracking. Similar processes do occur within the limestone, but due to its homogeneity, creep is constrained in calcite (monomineralic) and is associated with less damage increasing the time up to failure. It was also observed that both limestones that failed at a stress threshold above 0.8 UCS failed within the first 60 minutes. On the contrary, below CI threshold, no failure was observed, and between 0.5 to 0.8 UCS, failure will take place at some point between the first hours to months, depending on the rock type. Another outcome of this work was the identification of Maxwell's viscosity threshold as an indicator of failure. This observation can explain why some specimens fail and some others did not (yet).

Time-dependent behavior during tunneling can play an important role in the project success in the design and, most notably, in the construction process. This fourth dimension (time-effect) in tunneling was investigated numerically by performing an axisymmetric parametric analysis. From the research was concluded that current conventional methods adopted to predict the Longitudinal Displacement Profile of tunnel displacements have limited applications and fail to capture the overall displacement over time. It was also presented that both the excavation methods and excavation rate (tunnel advancement rate) can affect (deteriorate) the mechanical behavior of the surrounding rock mass. In this work, only creep behavior was considered a contributor to time-dependent deformation and was simulated with the modified purely visco-elastic CVISC model assuming the rock mass as a visco-elastic medium. It was further concluded that the retardation time (in the Kelvin-Voigt model) does control the timing at which the maximum tunnel displacement is reached during the primary stage of creep.


Finally, a new but yet simple tool that can be used to predict the long-term behavior of brittle materials as limestone using either the Long-Term Strength (LTS) approach (strength-degradation) and the Young's Modulus-Ratio (YMR) was presented. It should be stated that the proposed methodology should be used as a first estimate to relate the strength-deterioration of the rock material over time. Furthermore, input parameters can be derived in the plastic zone around an underground opening using this approach that can then be used in numerical analyses similar to the one presented herein.

## Author details

Chrysothemis Paraskevopoulou  
School of Earth and Environment, University of Leeds, Leeds, United Kingdom

\*Address all correspondence to: [c.paraskevopoulou@leeds.ac.uk](mailto:c.paraskevopoulou@leeds.ac.uk)

## IntechOpen

© 2021 The Author(s). Licensee IntechOpen. This chapter is distributed under the terms of the Creative Commons Attribution License (<http://creativecommons.org/licenses/by/3.0>), which permits unrestricted use, distribution, and reproduction in any medium, provided the original work is properly cited. 

## References

- [1] Paraskevopoulou, C., Vlachopoulos, N., Diederichs, M.S. 2012. Long-term behaviour and support analysis using numerical modeling, In: Proceedings of the 46th US Rock Mechanics – Geomechanics Symposium ARMA. June 2012, Chicago, USA.
- [2] Paraskevopoulou, C., Oke, J., Vlachopoulos, N. 2012. Practical modelling approaches to determine the long term behaviour of tunnel construction. In: Proceedings of the Canadian Tunnelling Symposium TAC on Tunnels and Underground Spaces: Sustainability and Innovations. September 2012, Montreal, Canada.
- [3] Paraskevopoulou, C., Diederichs, M.S. 2013. A comparison of viscous models under constant strain and constant stress: Implications for tunnel analysis. In: Proceedings of the World Tunnel Congress on Underground – the way to the future. June 2013, Geneva, Switzerland.
- [4] Paraskevopoulou, C., Diederichs, M.S. 2013. A comparison of viscous material model mechanics and impacts under different boundary conditions for tunnels and shafts. In: Proceedings of the 47th US Rock Mechanics – Geomechanics Symposium ARMA, June 2013, San Francisco, USA.
- [5] Paraskevopoulou, C., Benardos, A., 2012. Construction cost estimation for Greek road tunnels in relation to the geotechnical conditions, In: Proc. Int. Symp. Practices and Trends for Financing and Contracting Tunnels and Underground Works (Tunnel Contracts 2012), March 2012, Athens.
- [6] Paraskevopoulou, C., Benardos, A. 2013. Assessing the construction cost of tunnel projects. *Tunnelling and Underground Space Technology Journal*, 38(2013), 497-505. <https://doi.org/10.1016/j.tust.2013.08.005>
- [7] Benardos, A., Paraskevopoulou C., Diederichs, M., 2013. Assessing and benchmarking the construction cost of tunnels. In: Proceedings of 66th Canadian Geotechnical Conference, GeoMontreal on Geoscience for Sustainability, September 29–October 3, 2013, Montreal, Canada.
- [8] Paraskevopoulou C., Boutsis, G., Cost Overruns in Tunnelling Projects: Investigating the Impact of Geological and Geotechnical Uncertainty Using Case Studies. Special Issue Underground Infrastructure Engineering of Infrastructure Journal (MDPI). *Infrastructures* 2020, 5(9), 73; <https://doi.org/10.3390/infrastructures5090073>
- [9] Paraskevopoulou, C. 2016. Time-dependency of rock and implications associated with tunnelling, PhD Thesis. In: Queen's University Publications. Canada.
- [10] Weaver, S.H. 1936. Creep curve of steel. *Trans Amer Soc. Mech. Eng.*, LVIII, 745-751.
- [11] Griggs, D. 1939. Creep of Rocks. *Journal of Geology*. 47, 225-251
- [12] Bieniawski, Z.T. 1974. Geomechanics classification of rockmasses and its application in tunnelling. In: Proc. of the 3rd Congress, ISRM, Denver.
- [13] Barton, N.R., 1974. Estimating the shear strength of rock joints. In: Proc. of the 3rd Congress, ISRM. Denver.
- [14] Palmstrom, A. 1995. RMI-A rockmass characterization system for rock engineering purposes. Ph.D. Thesis. University of Oslo, Norway, 400 pages.
- [15] Widd, B.L. 1966. The time-dependent behaviour of rock; Considerations with regard to a research program. CSIR Report MEG 514,

Rock Mechanics Division, National Mechanical Engineering Research Institute, Pretoria, South Africa.

- [16] Bieniawski, Z.T. 1967. Mechanism of Brittle Fracture of Rock, parts I, II, and III. *Rock Mech. Min Sci*, 4 (4), 395-430.
- [17] Wawesik, W.R. 1972. Time-dependent rock behaviour in uniaxial compression. In: *Proc. of the 14th Rock Mechanics Symposium*, University of Pennsylvania, 85-106.
- [18] Singh, D.P. 1975. A study of creep of rocks. *Int. J. Rock Mech Sci & Geomech*, 12, 271-276.
- [19] Peng, S.S. 1973. Relaxation and the behaviour of failed rock. *Int. J. Rock Mech Min. Sci. & Geomech.*, 10, 235-246.
- [20] Kranz, R.L., and Scholz, C.H. 1977. Critical dilatant volume of rocks at the onset of tertiary creep. *J. Geophys. Res.*, 82 (4), 893-4,898.
- [21] Schmidtke, H., and Lajtai, E.Z. 1985. The long-term strength of Lac du Bonnet granite. *J. Rock Mech. Min. Sci. Geo.*, 22, 461-465.
- [22] Lau, J., Gorski B., Conlon, B., and Anderson, T. 2000. Long-term loading tests on saturated granite and granodiorite, Report: 06819-REP-01300-I 0016 ROO, CANMET, Natural Resources Canada.
- [23] Cristescu, N.,D. 2009. Time effects in rock mechanics. In *Proceedings of the SME Annual Conference*, Albuquerque, New Mexico.
- [24] Paraskevopoulou, C., Diederichs, M.S. 2013. Long-term behaviour in tunnelling: limitations in using creep parameters. In: *Proceedings of 66th Canadian Geotechnical Conference, GeoMontreal on Geoscience for Sustainability*, September 29–October 3, 2013, Montreal, Canada.
- [25] Paraskevopoulou, C., 2018. Predicting the long-term behaviour of rock masses in tunnelling. In: *Proceedings of the WTC 2018, Word Tunnelling Congress on The Role of Underground Space in Building Future Sustainable Cities*, April 2018, Dubai, United Emirates.
- [26] Paraskevopoulou, C., Perras, M., Diederichs, M.S., Loew, S., Lam, T., Jensen., M. 2018. Time-dependent behaviour of brittle rocks based on static load laboratory testing. *Geotechnical & Geological Engineering*, 36, 337-376(2018). <https://doi.org/10.1007/s10706-017-0331-8>
- [27] Bukharov, G.N., Chanda, M.W., and Bukharov, N.G. 1995. The three processes of brittle crystalline rock creep. *Int. J. Rock Mech. Min Sci. & Geomech*, 32 (4), 325-335.
- [28] Pellet, F., Hajdu, A., Deleruyelle, F. and Bensus, F. 2005. A visco-plastic model including anisotropic damage for the time-dependent behaviour of rock. *Int. J. for Num. Anal. Meth. Geomech.*, 29, 941-970.
- [29] Paraskevopoulou, C., Diederichs, M., 2018. Analysis of time-dependent deformation in tunnels using the Convergence-Confinement Method. *Tunnelling and Underground Space Technology Journal*, 71(2018), 62-80, 19 pages. <http://dx.doi.org/10.1016/j.tust.2017.07.001>
- [30] Innocente, J., Diederichs, M.S., Paraskevopoulou, C, Aubertin, J.D. 2020. Numerical investigation of the applicability of time-dependent creep models. Submitted to the: *Proceedings of the ISRM International Symposium – Eurock 2020 – Hard Rock Engineering*, June 2020, Trodheim, Norway.
- [31] Innocente, J., 2021. Time-dependency and long-term strength of rocks -limitations, interpretation and application in

finite difference continuum methods. MSc Thesis. In: Queen's University Publications. Canada.

[32] Paraskevopoulou, C., Perras, M., Diederichs, M.S., Amaan, F., Loew, S., Lam, T., 2015. Long-term static load laboratory testing behaviour of different rock types . In: Proceedings of the 68th Canadian Geotechnical Symposium GeoQuebec on Challenges from North to South. September 2015, Quebec, Canada.

[33] Paraskevopoulou, C., Perras, M., Diederichs, M.S., Amann, F., Loew, S., Lam, T., Jensen., M. 2017. The three stages of stress-relaxation - Observations for the long-term behaviour of rocks based on laboratory testing. *Journal of Engineering Geology*, 216, 56-75(2017). <http://dx.doi.org/10.1016/j.enggeo.2016.11.010>

[34] ASTM. 2013. Standard Test Methods for Stress Relaxation for Materials and Structures. E328-13. American Society for Testing and Materials.

[35] Paraskevopoulou, C., Perras, M., Diederichs, M.S., Amaan, F., Loew, S., Lam, T., 2015. Observations for the long-term behaviour of carboniferous limestone rocks based on laboratory testing. In: Proceedings of the EUROCK 2015 Future Development of Rock Mechanics – 64th Geomechanics Colloquium, October 2015, Salzburg, Austria.

[36] Paraskevopoulou, C., Perras, M.A., 2017. Investigating the long-term behaviour of brittle rocks: Visco-elastic creep parameters and time-to-failure. In: PRF 2017: Progressive Failure and Long-term Strength Degradation of Brittle Rocks ISRM Conference, June 2017, Ascona, Switzerland.

[37] ISRM. 2014. Suggested methods for determining the creep characteristics of rock.47, 275-290

[38] Goodman, R.E. 1980. Introduction to Rock Mechanics, John Wiley and Sons, New York.

[39] Davis, G.H., Reynolds, S.J., and Kluth, C.F. 2012. Structural Geology of Rocks and Regions. 3rd Edition. Wiley. New York. (ISBN:978-1-118-21505-0), 864 pages.

[40] Fairhurst, C., and Cook, N.G.W. 1966. The phenomenon of rock splitting parallel to the direction of maximum compression in the neighborhood of a surface. In: Proc. of the First Congress on the International Society of Rock Mechanics, National Laboratory of Civil Engineering, Lisbon, Portugal, 1, 687-692.

[41] Diederichs, M.S., Day, J.J., Ghazvinian, E., Perras, M., Paraskevopoulou, C., Walton, G., Progressive brittle damage processes and failure in rock. Keynote Lecture in the Progressive Failure and Long-term Strength Degradation of Brittle Rocks In: PRF 2017: Progressive Failure and Long-term Strength Degradation of Brittle Rocks. ISRM Conference, June 2017, Ascona, Switzerland.

[42] ISRM. 1979. Suggested methods for determining the uniaxial compressive strength and deformability of rock materials. 16, 2, 138-140.

[43] Martin, C.D. 1997. Seventeenth Canadian Geotechnical Colloquium: The effect of cohesion loss and stress path on brittle rock strength. *Can. Geotech. J.*, 34 (5), 698-725.

[44] Martin, C.D. 1993. The Strength of massive Lac du Bonnet granite around underground openings. Ph.D. Thesis. University of Manitoba, Canada.

[45] Martin, C.D., Kaiser, P.K., and McCreath, D.R. 1999. Hoek-Brown parameters for predicting the depth of brittle failure around tunnels. *Can. Geotech. J.*, 36 (1), 136-151.

- [46] Perras, M.A., and Diederichs, M.S. 2014. A review of the Tensile Strength of Rock: Concepts and Testing. *J. Geotech. and Geol. Eng.*, 32, 525-546.
- [47] Gorski, B., Anderson, T., and Conlon, B. 2009. DGR site characterization documents, technical reports TR-08-11. Available at [www.nwmo.ca].
- [48] Gorski, B., Anderson, T., and Conlon, B. 2010. DGR site characterization documents, technical reports TR-08-36. Available at [www.nwmo.ca].
- [49] Diederichs, M.S. 2003. Rock fracture and collapse under low confinement conditions. *Rock Mech. Rock Eng.*, 36 (5), 339-381.
- [50] Panet, M. 1995. *Calcul des Tunnels par la Méthode de Convergence-Confinement*. Presses de l'Ecole Nationale des Ponts et Chaussées, Paris, 178 pages.
- [51] Panet, M. 1979. Time-dependent deformations in underground works. In: *Proc. of the 4th Int Congress on Rock Mechanics*, Montreux.
- [52] Sulem, J., Panet, M. and Guenot, A. 1987. Closure analysis in deep tunnels and Analytical solution for time-dependent displacement in a circular tunnel. *Int. J. Rock Mech. & Min. Sci. & Geom. Abstracts*. 24(3), 145-154 and 155-164.
- [53] Paraskevopoulou, C., Diederichs, M.S., 2017. How time-dependency influences the Longitudinal Displacement Profile during the construction of deep tunnels. In: *Proceedings of the WTC 2017, World Tunnelling Congress on Surface Challenges – Underground Solutions*, June 2017, Bergen, Norway.
- [54] Paraskevopoulou, C., Diederichs, M.S., Perras, M. 2017. Time-dependent rock masses and implications associated with tunnelling, In: *Proceedings of EUROTUN 2017, IV International Conference on Computational Methods in Tunnelling and Subsurface Engineering*, April 2017, Innsbruck, Austria.